

Search for extra dimensions in diphoton events from proton–proton collisions at $\sqrt{s} = 7$ TeV in the ATLAS detector at the LHC

The ATLAS Collaboration

New Journal of Physics **15** (2013) 043007 (34pp)

Received 21 February 2013

Published 4 April 2013

Online at <http://www.njp.org/>

doi:10.1088/1367-2630/15/4/043007

E-mail: atlas.publications@cern.ch

Abstract. The large difference between the Planck scale and the electroweak scale, known as the hierarchy problem, is addressed in certain models through the postulate of extra spatial dimensions. A search for evidence of extra spatial dimensions in the diphoton channel has been performed using the full set of proton–proton collisions at $\sqrt{s} = 7$ TeV recorded in 2011 with the ATLAS detector at the CERN Large Hadron Collider. This dataset corresponds to an integrated luminosity of 4.9 fb^{-1} . The diphoton invariant mass spectrum is observed to be in good agreement with the Standard Model expectation. In the context of the model proposed by Arkani–Hamed, Dimopoulos and Dvali, 95% confidence level lower limits of between 2.52 and 3.92 TeV are set on the ultraviolet cutoff scale M_S depending on the number of extra dimensions and the theoretical formalism used. In the context of the Randall–Sundrum model, a lower limit of 2.06 (1.00) TeV at 95% confidence level is set on the mass of the lightest graviton for couplings of $k/\overline{M}_{\text{Pl}} = 0.1(0.01)$. Combining with the ATLAS dilepton searches based on the 2011 data, the 95% confidence level lower limit on the Randall–Sundrum graviton mass is further tightened to 2.23 (1.03) TeV for $k/\overline{M}_{\text{Pl}} = 0.1(0.01)$.

Contents

1. Introduction	2
2. The ATLAS detector	4
3. Trigger and event selection	4
4. Event simulation	5
5. Background estimate	6
6. Systematic uncertainties in the signal models	9
7. Results and interpretation	11
8. Summary	14
Acknowledgments	15
References	33

1. Introduction

One of the major goals of particle physicists in past decades has been to solve the hierarchy problem: the fact that the electroweak scale is 16 orders of magnitude smaller than the Planck scale. One possible solution to the hierarchy problem is the existence of extra spatial dimensions. In this paradigm, gravity appears much weaker than the other interactions because it is diluted by the presence of extra spatial dimensions.

In the Randall–Sundrum (RS) model [1], a five-dimensional geometry is assumed, in which the fifth dimension is compactified with length r_c . There are two four-dimensional branes sitting in a five-dimensional bulk with a ‘warped’ geometry. The Standard Model (SM) fields are located on the so-called TeV brane, while gravity originates from the other brane, called the Planck brane. Gravitons are capable of propagating in the bulk. Mass scales on the TeV brane correspond to mass scales on the Planck brane (M_{Pl}) as given by $M_D = M_{\text{Pl}} e^{-k\pi r_c}$, where k is the curvature scale of the extra dimension. The observed hierarchy of scales can be naturally reproduced in this model if $kr_c \approx 12$ [2]. The compactification of the extra dimension gives rise to a Kaluza–Klein (KK) tower of graviton excitations G , a set of four-dimensional particles with increasing masses. The phenomenology can be described in terms of the mass of the lightest KK graviton excitation (m_G) and the dimensionless coupling to the SM fields, $k/\overline{M}_{\text{Pl}}$, where $\overline{M}_{\text{Pl}} = M_{\text{Pl}}/\sqrt{8\pi}$ is the reduced Planck scale. From theoretical arguments [2], $k/\overline{M}_{\text{Pl}}$ values in the range $[0.01, 0.1]$ are preferred. The lightest RS graviton is expected to be a fairly narrow resonance for $k/\overline{M}_{\text{Pl}} < 0.3$. The most stringent experimental limits on RS gravitons have been obtained at the LHC: the current best 95% confidence level (CL) lower limits on the graviton mass for $k/\overline{M}_{\text{Pl}} = 0.1$ are 2.16 TeV [3] and 2.14 TeV [4]. The former limit has been obtained from an analysis of the $G \rightarrow ee/\mu\mu$ channels in data corresponding to an integrated luminosity of 5 fb^{-1} collected by the ATLAS experiment. The latter limit has been obtained from an analysis of the same channels in data corresponding to an integrated luminosity of $\approx 5 \text{ fb}^{-1}$ collected by the CMS experiment. The limits from earlier searches at the Tevatron can be found in [5, 6].

Arkani–Hamed, Dimopoulos and Dvali (ADD) [7] proposed a different scenario for extra dimensions. Motivated by the weakness of gravity, they postulated the existence of n flat additional spatial dimensions compactified with radius R , and proposed a model in which

only gravity propagates in the extra dimensions. The fundamental Planck scale in the $(4+n)$ -dimensional spacetime, M_D , is related to the apparent scale \overline{M}_{Pl} by Gauss's law: $\overline{M}_{\text{Pl}}^2 = M_D^{n+2} R^n$. The mass splitting of the graviton KK modes is $1/R$ for each of the n extra dimensions. In the ADD model, resolving the hierarchy problem usually requires small values of $1/R$, giving rise to an almost continuous spectrum of KK graviton states. The symbol G is used to denote KK graviton states in both the RS and ADD models. The existence of ADD extra dimensions can manifest itself in proton–proton (pp) collisions through a variety of processes, including virtual graviton exchange as well as direct graviton production. While processes involving direct graviton emission depend on M_D , effects involving virtual gravitons depend on the ultraviolet cutoff of the KK spectrum, denoted M_S . The strength of gravity in the presence of extra dimensions is typically parametrized by $\eta_G = F/M_S^4$, where F is a dimensionless parameter of the order of unity reflecting the dependence of virtual KK graviton exchange on the number of extra dimensions. Several theoretical formalisms exist in the literature, using different definitions of F and, consequently, of M_S :

$$F = 1 \quad (\text{GRW}) [8], \quad (1)$$

$$F = \begin{cases} \log(M_S^2/\hat{s}) & n = 2 \\ 2/(n-2) & n > 2 \end{cases} \quad (\text{HLZ}) [9], \quad (2)$$

$$F = \pm 2/\pi \quad (\text{Hewett}) [10], \quad (3)$$

where $\sqrt{\hat{s}}$ is the centre-of-mass energy of the parton–parton collision. The effect of ADD graviton exchange manifests itself as a non-resonant deviation from the SM background expectation. The effective diphoton cross section is the result of the SM and ADD amplitudes, as well as their interference. The interference term in the effective cross section is linear in η_G and the pure graviton exchange term is quadratic in η_G . In previous analyses by the ATLAS and CMS collaborations, 95% CL lower limits on M_S of 2.26–3.52 TeV [11] and 2.4–3.8 TeV [12], respectively, were set, depending on the theoretical formalism used. Searches for ADD virtual graviton effects have also been performed at other colliders, e.g. at HERA [13, 14], LEP [15–17] and the Tevatron [18, 19].

This paper reports the results of a search for extra dimensions in the diphoton channel using the full data sample recorded by the ATLAS detector in 2011, corresponding to a total integrated luminosity of 4.9 fb^{-1} of pp collisions at $\sqrt{s} = 7 \text{ TeV}$. The results are interpreted in the context of both the ADD and RS scenarios. The dilepton and diphoton channels are particularly sensitive for this search due to the clean experimental signature, excellent mass resolution and modest backgrounds. The branching ratio for graviton decay to two photons is twice the value of the branching ratio for graviton decay to any individual charged-lepton pair. This search, based on the full $\sqrt{s} = 7 \text{ TeV}$ 4.9 fb^{-1} dataset, is an extension of an earlier study [11] that was performed using $1.0\text{--}2.1 \text{ fb}^{-1}$ of data. The earlier data are included in the present study, but they benefit from improvements in the reconstruction and calibration procedures. Moreover, the techniques used for the background estimation and their associated uncertainties have also been significantly improved. This results in an overall improvement of a factor of 2–3 in the excluded production cross section of diphoton events predicted by the RS model, corresponding to a graviton mass limit which is 10–15% larger.

2. The ATLAS detector

The ATLAS detector is a multipurpose particle physics instrument with a forward–backward symmetric cylindrical geometry and near 4π solid angle coverage¹. A detailed description of the ATLAS detector can be found in [20]. The inner tracking detector (ID) consists of a silicon pixel detector, a silicon microstrip detector and a transition radiation tracker. The ID is surrounded by a superconducting solenoid that provides a 2 T axial magnetic field. The ID allows an accurate reconstruction of tracks from the primary pp collision and also identifies tracks from secondary vertices, permitting the efficient identification of photon conversions.

The electromagnetic calorimeter (ECAL) is a lead/liquid-argon (LAr) sampling calorimeter with an accordion geometry. It is divided into a barrel section, covering the pseudorapidity² region $|\eta| < 1.475$, and two endcap sections, covering the pseudorapidity regions $1.375 < |\eta| < 3.2$. It consists of three longitudinal layers for $|\eta| < 2.5$ and two for $2.5 < |\eta| < 3.2$. Up to $|\eta| < 2.4$, the first one uses highly granular ‘strips’ segmented in the η direction for efficient event-by-event discrimination between single photon showers and two overlapping showers originating from π^0 decay. The second layer collects most of the energy deposited in the ECAL by photon showers. Significant energy deposits in the third layer are an indication of leakage beyond the ECAL from a high energy shower. The measurements from the third layer are used to correct for this effect. A thin presampler layer in front of the accordion calorimeter, covering the pseudorapidity interval $|\eta| < 1.8$, is used to correct for the energy loss upstream of the calorimeter.

The hadronic calorimeter, surrounding the ECAL, includes a central ($|\eta| < 1.7$) iron/scintillator tile calorimeter, two endcap ($1.5 < |\eta| < 3.2$) copper/LAr calorimeters and two forward calorimeters that extend the coverage to $|\eta| < 4.9$, using copper and tungsten as the absorber. The muon spectrometer, located beyond the calorimeters, consists of three large air-core superconducting toroid systems, instrumented with precision tracking chambers as well as fast detectors for triggering.

3. Trigger and event selection

The analysis uses data recorded by ATLAS between March and October 2011 during stable-beam periods of pp collisions at $\sqrt{s} = 7$ TeV. A three-level trigger system is used to select events containing two photon candidates. The first-level trigger is hardware-based and relies on a readout with coarse granularity. The second- and third-level triggers, collectively referred to as the high-level trigger (HLT), are implemented in software and exploit the full granularity and energy calibration of the calorimeter. Selected events have to satisfy a diphoton trigger where each photon is required to satisfy, at the HLT level, a transverse energy requirement $E_T^\gamma > 20$ GeV and a set of requirements [21, 22] on the shape of the energy deposit. This set includes criteria for the energy leakage into the hadronic calorimeter and for the width of the shower in the second layer of the ECAL. This trigger is nearly 100% efficient for diphoton events passing the final selection requirements.

¹ ATLAS uses a right-handed coordinate system with its origin at the nominal interaction point (IP) in the centre of the detector and the z -axis along the beam pipe. The x -axis points from the IP to the centre of the LHC ring, and the y -axis points upward. Cylindrical coordinates (r, ϕ) are used in the transverse plane, ϕ being the azimuthal angle around the beam pipe.

² The pseudorapidity is defined in terms of the polar angle θ as $\eta = -\ln \tan(\theta/2)$.

Only events satisfying the standard ATLAS data quality requirements and having at least one primary collision vertex with at least three tracks are kept. Photon candidates reconstructed in the precision regions of the barrel ($|\eta| < 1.37$) or the endcaps ($1.52 < |\eta| < 2.37$), with $E_T^\gamma > 25$ GeV and satisfying the same requirements on the shower shape as the trigger, are preselected. These requirements on the photon candidates are referred to as the loose selection. The two highest- E_T^γ photon candidates each have to satisfy a set of stricter requirements, referred to as the tight photon definition, which includes a more stringent selection on the shower width in the second layer of the ECAL and additional requirements on the energy distribution in the first layer of the ECAL. In addition, the two photon candidates of interest have to satisfy a calorimetric isolation requirement, $E_T^{\text{iso}} < 5$ GeV. This isolation is computed by summing the transverse energy over the cells of the calorimeters in a cone of radius $\Delta R = \sqrt{(\eta - \eta^\gamma)^2 + (\phi - \phi^\gamma)^2} < 0.4$ surrounding the photon candidate. Here (η, ϕ) denotes the cell position and $(\eta^\gamma, \phi^\gamma)$ denotes the position of the photon cluster [23]. The transverse energy contribution in the centre of the cone, which contains the photon cluster, is subtracted. Corrections, based on simulations, are applied to account for the expected energy leakage from the photon into the isolation region. An ambient-energy correction, based on the measurement of low-transverse-momentum jets [24], is also applied, on an event-by-event basis, to remove the contributions from the underlying event and from pile-up which results from the presence of multiple pp collisions within the same or nearby bunch crossings.

4. Event simulation

Monte Carlo (MC) simulations are used to study the response of the detector to various RS and ADD scenarios as well as SM diphoton processes. The MC generators used in this analysis are listed below. For samples generated using PYTHIA [25], the ATLAS parameter tunes [26] are used in the event generation. For samples generated using PYTHIA or SHERPA [27], the generated events are processed through the GEANT4 [28] detector simulation [29]. Then the simulated events are reconstructed with the same procedure as is used for the data. To reproduce the pile-up conditions of the data, the simulated events are reweighted to match the observed distribution of the average number of interactions per bunch crossing. The determination of the number of interactions per bunch crossing is discussed in [30].

PYTHIA 6.424 with MRST2007LOMOD [31] parton distribution functions (PDFs) is used to simulate the SM diphoton production at leading order (LO). In addition, the next-to-leading (NLO) correction and the contribution of the fragmentation processes are evaluated using DIPHOX [32] 1.3.2 with MSTW2008NLO [33] PDFs and lead to an invariant-mass-dependent correction of the PYTHIA prediction. The so-called box contribution $gg \rightarrow \gamma\gamma$ through a quark loop is included in both the PYTHIA and the DIPHOX predictions. From the point of view of power counting, this diagram is a next-to-next-to-leading contribution, but the gluon luminosity at the LHC is so large compared to the quark–antiquark one that this process represents a contribution that is comparable to the $q\bar{q} \rightarrow \gamma\gamma$ process. Samples of RS events are produced using the same generator and PDFs as for the SM diphoton samples. They are used to study the selection efficiency and the shape of the reconstructed invariant mass spectrum for various values of the graviton mass m_G between 400 and 3000 GeV and values of $k/\overline{M}_{\text{Pl}}$ in the range $[0.01, 0.1]$. ADD models are simulated for various M_S values using SHERPA 1.3.1 with CTEQ6L [34] PDFs. The ADD MC samples are used to evaluate the number of signal events passing the selection as a function of M_S . An NLO K -factor of 1.75 ± 0.10 is considered for the RS scenario and

1.70 ± 0.10 is considered for the ADD scenario. These K -factors have been provided by the authors of [35, 36].³

5. Background estimate

The dominant background in this analysis is the irreducible background due to SM $\gamma\gamma$ production. Another significant background component is the reducible background which arises from events in which one or both of the photon candidates result from a different object being misidentified as a photon. This background is dominated by $\gamma + \text{jet}$ (j) and $j + j$ events, with one or both photon candidates arising from jets. Backgrounds with electrons faking photons, such as the Drell–Yan production of electron–positron pairs as well as $W/Z + \gamma$ and $t\bar{t}$ processes, have been verified to be negligible after the event selection.

We first describe the tools and samples that are used to predict the contributions from the SM $\gamma\gamma$ background to the high-mass signal region, as well as their main limitation. We then describe in detail the two-step procedure that is used to overcome this limitation and to obtain our background estimate.

The estimate of the irreducible background makes use of the NLO calculations [32] that are available for the SM $\gamma\gamma$ production processes. The uncertainty in the absolute normalization of the $\gamma\gamma$ cross section is, however, quite substantial: $\simeq 20\%$ ($\simeq 25\%$) uncertainty on the cross section for $\gamma\gamma$ events with an invariant mass $m_{\gamma\gamma} > 200 \text{ GeV}$ ($m_{\gamma\gamma} > 1200 \text{ GeV}$) with both photons in the detector acceptance. The background estimates, which are discussed in detail below, are therefore normalized to the data in the low-mass control region⁴ ([142, 409] GeV) where the presence of any signal beyond the SM has been excluded by previous searches. Compared to the use of NLO calculations to predict the absolute rate of SM $\gamma\gamma$ production in the high-mass signal region, the use of NLO calculations for the extrapolation of the SM $\gamma\gamma$ production rates from the low-mass control region to the high-mass signal region results in significantly smaller uncertainties. The extrapolation method is described in detail below, along with quantitative estimates of the final uncertainties.

Following these considerations, the estimation of the $m_{\gamma\gamma}$ spectrum of the background events is done in two steps. First, the shape of the $m_{\gamma\gamma}$ spectrum is determined separately for each background component. Then, the normalization for each component is determined using the low-mass control region.

The shape of the $m_{\gamma\gamma}$ spectrum from SM $\gamma\gamma$ production is estimated using simulated events, reweighting the PYTHIA samples to the differential (in $m_{\gamma\gamma}$) cross section predicted using DIPHOX.

The shape of the reducible background is estimated using data-driven techniques. It is split into three components: $\gamma + j$ events (the leading- E_T photon candidate is due to a real photon), $j + \gamma$ (fake leading photon candidate) and $j + j$. The shapes of the $j + \gamma$ and $\gamma + j$ differ significantly because of the strong p_T -dependence of the probability of misidentifying a jet as a photon. Separately for each component, several data control samples that are enriched in the given component are defined. The shape of the $\gamma + j$ background is estimated from a data

³ Including updated calculations at this collision energy.

⁴ The exact values of the upper and lower bounds of the low-mass control region have been chosen to coincide with the boundaries of the first bin in table 1. The results of this search are not altered either by small variations of the control region edges or by a change of the binning.

control sample that is selected in the same way as the signal sample, except that the subleading γ candidate is required to pass loose identification criteria and to fail tight identification criteria. The control samples used to extract the shapes of the $m_{\gamma\gamma}$ spectra of $j + \gamma$ and $j + j$ backgrounds are defined following the same approach, i.e. by requiring the leading photon candidate ($j + \gamma$ background) or both candidates ($j + j$ background) to pass loose and to fail tight identification criteria. Since the data control samples contain relatively few events at high $m_{\gamma\gamma}$, a fit to a smooth function of the form $f(m_{\gamma\gamma}) = p_1 \times (m_{\gamma\gamma})^{p_2 + p_3 \log m_{\gamma\gamma}}$, where the p_i are free parameters, is used to extrapolate the reducible background shapes to higher masses. This functional form has been used in the CDF dijet search [37] and in previous ATLAS searches in the dilepton [38], dijet [39], photon-jet [40] and diphoton [11] channels, and it describes the shapes of the data control samples well. In contrast to the earlier version of this analysis [11], the shapes of the three components of the reducible background are modelled separately.

To determine the contributions of each of the four sources (the irreducible $\gamma\gamma$ component plus the three reducible components, $\gamma + j$, $j + \gamma$ and $j + j$) to the low-mass control region, a two-dimensional template fit to the distributions of the calorimetric isolation (E_T^{iso}) of the two photon candidates is used. For the purpose of this fit, the isolation requirement in the event selection is relaxed to $E_T^{\text{iso}} < 25$ GeV. This method has been used previously in [41, 42] and in an earlier version of this analysis [11]. Templates for the E_T^{iso} distribution of true photons and of fake photons from jets are both determined from data. The shape for fake photons is determined using a sample of photon candidates that fail the tight requirement but pass a set of requirements referred to as the non-tight selection. This non-tight selection includes the same requirements as the loose selection plus additional requirements that reduce the correlation between the identification and the isolation. The shape for true photons is found from the sample of tight photon candidates, after subtracting the fake photon shape normalized to match the number of candidates with large values of E_T^{iso} ($E_T^{\text{iso}} > 10$ GeV; this control region is dominated by fake photons). Both the signal templates and fake templates are constructed separately for leading and subleading photon candidates. The significant correlation ($\sim 20\%$) between the E_T^{iso} values of the two fake photons in the $j + j$ background is included in the two-dimensional template for this background component. The background expectation as a function of $m_{\gamma\gamma}$ is summarized in figure 1 and table 1. Figure 2 details the different contributions to the uncertainty in the background expectation.

The uncertainties in the shape of the irreducible background are dominated by the uncertainties in the PDFs that are used with DIPHOX. Those uncertainties are evaluated using the MSTW2008 NLO eigenvector PDF sets and using CTEQ6.6 and MRST2007LOMOD PDF sets for comparisons. The spread of the variations includes the difference between the central values obtained with the different PDF sets. Smaller contributions arise from residual imperfections in the simulation of the isolation variable E_T^{iso} and from higher-order contributions that are not included in the DIPHOX model. The latter contribution is evaluated by varying in a coherent and an incoherent way the renormalization, the initial factorization and the final factorization scales by a factor of 2 around their nominal value, which is the invariant mass of the diphoton system. The shape predictions from DIPHOX are found to be in good agreement with those obtained using an alternative NLO generator, MCFM [44] (with the same PDF set as DIPHOX). The small difference between the two generators is assigned as an additional systematic uncertainty. It represents a negligible contribution for $m_{\gamma\gamma} > 1$ TeV. The uncertainties in the shape of the reducible background arise from the finite size of the background control samples, and from the extrapolation of the background shapes from the control sample to the signal region. The

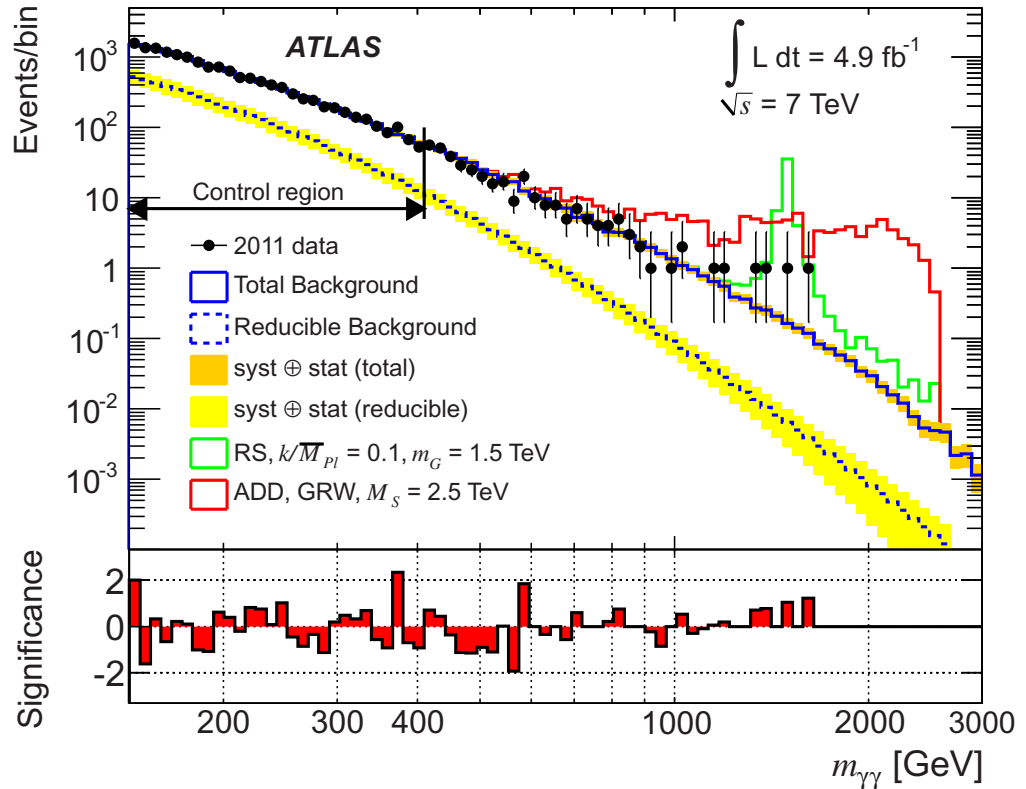


Figure 1. The observed invariant mass distribution of diphoton events. Superimposed are the SM background expectation and the expected signals for an example each for RS and ADD models. In addition to the total background, the contribution from the reducible component is shown. The black arrow indicates the control region. To compensate for the rapid decrease of the spectrum, the bins have been chosen to have constant logarithmic width. Specifically, the ratio of the upper to lower bin boundary is equal to 1.038 for all bins, and the first bin starts at 142 GeV. The bin-by-bin significance of the difference between the data and the predicted background is shown below the main plot. Following the convention of [43], the significance is set to zero for bins with insignificant deviations with respect to a small expected background. This concerns mainly the bins at large $m_{\gamma\gamma}$ where a fraction of an event is expected (on average) and where zero events are observed.

latter are assessed by varying the definition of the loose selection requirement which is used to define the control samples. The shape uncertainty of the reducible background has a small impact on the total background (figure 2). This is mainly because the reducible background is a small contribution to the total (table 1). The uncertainties in the normalization of the background components are dominated by the uncertainties in the templates used in the fit to the E_T^{iso} distributions. The uncertainties in the templates are assessed by varying the definition of the non-tight selection requirement used in the extraction of the templates. They are then propagated to the normalizations by repeating the template fits with the varied templates.

Table 1. The expected numbers of events from the irreducible and reducible background components, as well as the total background prediction and observed numbers of events in $m_{\gamma\gamma}$ bins. The table quotes the sum of the statistical and systematic uncertainties in the background expectations. The boundaries of all bins in this table have been chosen to coincide with bin boundaries in figure 1. As discussed in the text, the background estimate is normalized to the data in the low-mass control region [142, 409] GeV. Since the uncertainties in the normalization are strongly anticorrelated between the reducible and irreducible components, their impact on the estimate of the total background is smaller than their impact on the individual components. By construction, the uncertainties in the control region are 100% anticorrelated and the total background expectation is identical to the number of observed events.

Mass window (GeV)	Background expectation			Observed events
	Irreducible	Reducible	Total	
[142, 409]				
Control region	10 195 \pm 1092	4586 \pm 1092	14 781	14 781
[409, 512]	192 \pm 26	43 \pm 10	235 \pm 20	221
[512, 596]	57 \pm 8	10.7 \pm 2.7	68 \pm 7	62
[596, 719]	35 \pm 5	5.4 \pm 1.5	40 \pm 4	38
[719, 805]	12.0 \pm 1.8	1.4 \pm 0.4	13.3 \pm 1.6	13
[805, 901]	7.8 \pm 1.2	0.70 \pm 0.23	8.5 \pm 1.1	10
[901, 1008]	4.6 \pm 0.7	0.35 \pm 0.13	5.0 \pm 0.7	2
[1008, 1129]	2.7 \pm 0.4	0.18 \pm 0.07	2.8 \pm 0.4	2
[1129, 1217]	1.14 \pm 0.18	0.064 \pm 0.028	1.21 \pm 0.18	2
[1217, 1312]	0.72 \pm 0.12	0.040 \pm 0.018	0.76 \pm 0.11	0
[1312, 1414]	0.50 \pm 0.08	0.024 \pm 0.012	0.53 \pm 0.08	2
[1414, 1644]	0.61 \pm 0.10	0.024 \pm 0.013	0.63 \pm 0.10	2
[1644, 2889]	0.39 \pm 0.08	0.013 \pm 0.009	0.40 \pm 0.07	0

6. Systematic uncertainties in the signal models

Experimental systematic uncertainties on the signal yields are evaluated for both the RS and the ADD signals. The main systematic uncertainties arise from the non-perfect simulation of the quantities used for the identification of photons and in the isolation requirements. For the former, the data-driven estimates from [22] are used, together with an extrapolation to larger values of p_T , which are relevant in the present search. In the RS scenario, these uncertainties on the photon identification translate into a relative uncertainty of 4.7–3.3% on the signal yield for m_G values of 0.5–2.5 TeV. In the ADD scenario, the relative uncertainty on the signal yield is 4.5% with a weak dependence on M_S . For the latter, a study comparing the data sample and the simulation has shown that a 1 GeV shift of the isolation distribution in the simulation covers possible discrepancies between the data and the simulation in the signal region. In the RS scenario, these uncertainties translate into a relative uncertainty of 4–7% on the signal yield for m_G values of 0.5–2.5 TeV. In the ADD scenario, the relative uncertainty on the signal yield is $\sim 6\%$ with a weak dependence on M_S . The uncertainty on the integrated luminosity for the complete 2011

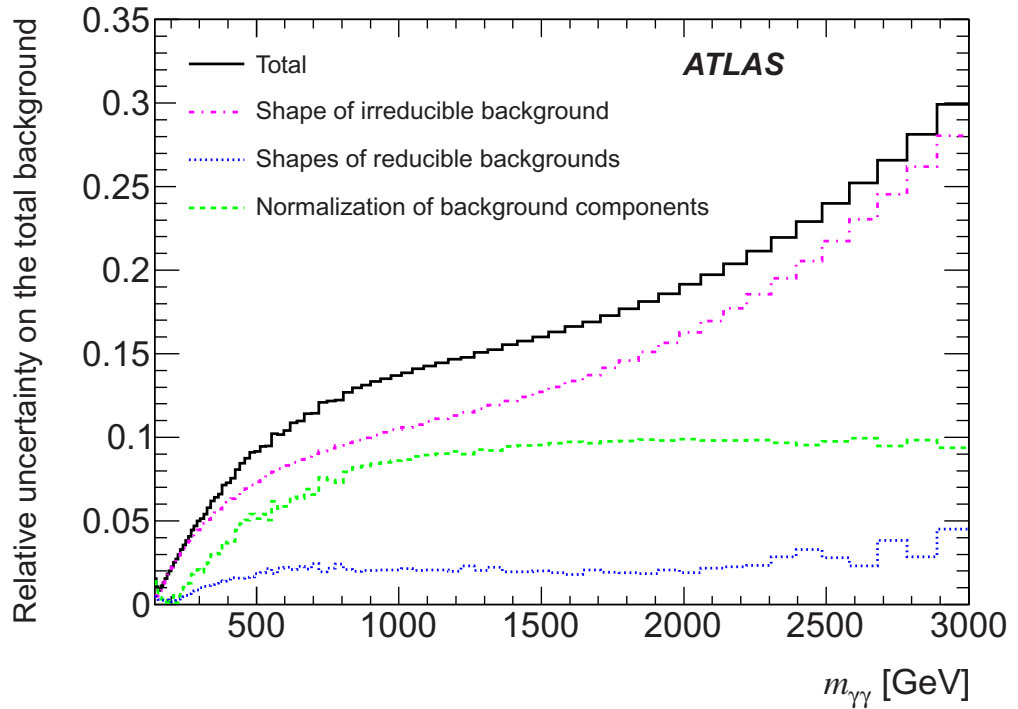


Figure 2. Uncertainty in the total background expectation as a function of $m_{\gamma\gamma}$. Also shown are the individual contributions from the uncertainties in the shapes of the irreducible and the reducible components, as well as the contribution from the uncertainties in the yields (normalizations) of the different background components extracted from the low-mass control region. Since the number of events in the low-mass control region is dominated by the lowest masses, the background uncertainties are particularly small at the low end of the control region.

dataset is 3.9%, based on the calibration described in [30, 45] plus an additional uncertainty for the extrapolation to the later data-taking period with a higher instantaneous luminosity. An uncertainty of 2% on the trigger efficiency arises from the differences between the measured trigger efficiency in the data and simulated samples. Given that the sum in quadrature of all experimental systematic uncertainties depends only weakly on the signal scenario, a common relative uncertainty value of 9% on signal yield is used for all scenarios.

Uncertainties from limited MC sample sizes, as well as uncertainties in the RS resonant shape due to the current knowledge of the electromagnetic energy scale of the calorimeter, the resolution of the detector and the pile-up conditions, were verified to have negligible impact on the result. Theoretical uncertainties due to the PDFs and due to uncomputed higher perturbative orders were considered. The uncertainty in the PDFs translates into an uncertainty of $^{+10}_{-5}\%$ in the signal yields predicted by the ADD models. In the RS scenario the PDF uncertainty in the signal yield is between 6 and 25% for m_G values between 0.5 and 2.5 TeV. As detailed in [11], an uncertainty of ± 0.1 is considered on the NLO K -factor value. The theory uncertainties are not included in the limit calculation, but their size is indicated in figures 3 and 5, where graphical representations of the limits discussed in section 7 are shown.

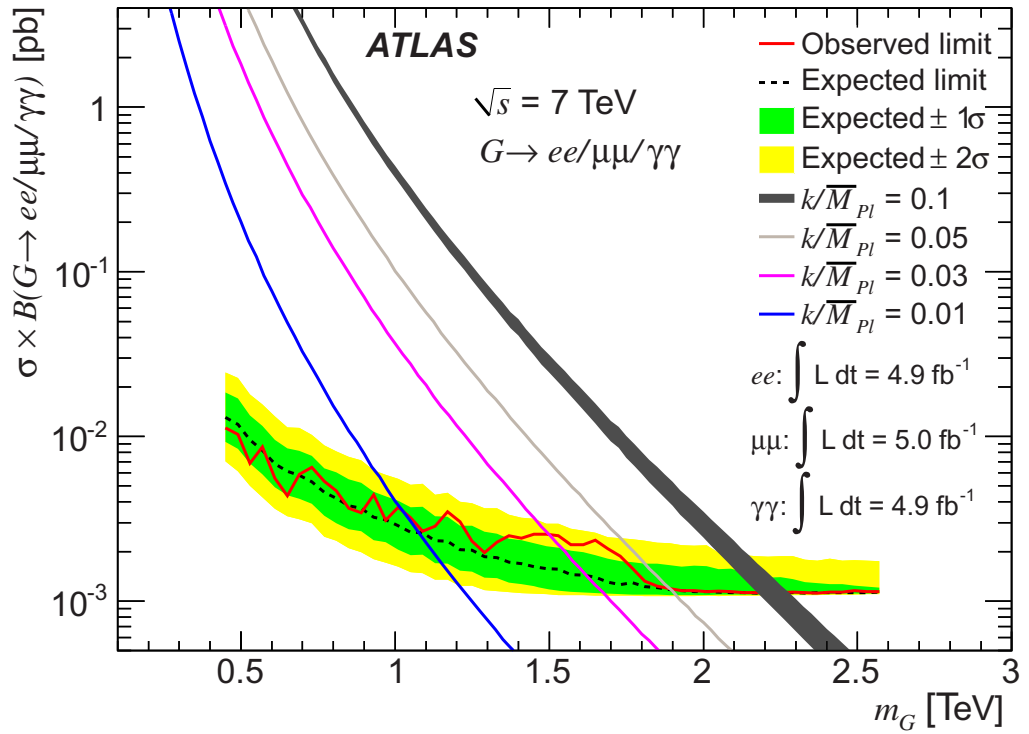


Figure 3. The expected and observed 95% CL limits from the combination of $G \rightarrow \gamma\gamma/ee/\mu\mu$ channels on $\sigma \times B$, the product of the RS graviton production cross section and the branching ratio for graviton decay via $G \rightarrow \gamma\gamma/ee/\mu\mu$, as a function of the graviton mass. The -1σ and -2σ variations of the expected limit exhibit a tendency to be particularly close to the expected limit at large m_G . This behaviour is expected as signals with large m_G would manifest themselves in regions of $m_{\gamma\gamma}$ where the SM background is small and the Poissonian fluctuations around the mean expected background are highly asymmetric. The theory curves are obtained using the PYTHIA generator, which implements the calculations from [48]. A K -factor of 1.75 is applied on top of these predictions to account for NLO corrections. The thickness of the theory curve for $k/\overline{M}_{Pl} = 0.1$ illustrates the theoretical uncertainties due to the PDFs expressed at 90% CL.

7. Results and interpretation

A comparison of the observed invariant mass spectrum of diphoton events and the background expectation is shown in figure 1, along with the statistical significance of the bin-by-bin difference [43] between the data and the expected background. This significance is plotted as positive (negative) for bins with an excess (deficit) of data. Also shown are the expected signals for two examples of RS and ADD models. The geometrical acceptance for the RS scenario with $m_G = 1.5$ TeV and $k/\overline{M}_{Pl} = 0.1$ shown in figure 1 is 88% and the selection efficiency for events within the acceptance is $(54 \pm 5)\%$. Both figure 1 and table 1 show that, over the entire $m_{\gamma\gamma}$ range, the data are in good agreement with the expectations from SM backgrounds. The BUMPHUNTER algorithm [46] is used to further quantify the level of agreement between the data and the SM background expectation. The BUMPHUNTER performs a scan of the mass

spectrum in windows of progressively increasing width. It identifies the window with the most significant excess of data events over the background expectation anywhere in a predefined search region. In this analysis, the binned mass spectrum of figure 1 is used, the search region is defined as $142 < m_{\gamma\gamma} < 3000$ GeV and the window size is allowed to vary from one bin to half the number of bins in the search region⁵. The most significant excess is found in the region $1312 < m_{\gamma\gamma} < 1644$ GeV. The probability of observing, due to fluctuations in the background alone, an excess that is at least as significant as that in the data is 0.86. This confirms the absence of a significant excess in the mass spectrum.

Given the absence of evidence for a signal, 95% CL upper limits were determined on the RS signal cross section. The limits are computed using a Bayesian approach [47] assuming a flat prior for the RS cross section. The likelihood function is defined as the product of the Poisson probabilities over all the mass bins in the search region defined as $m_{\gamma\gamma} > 409$ GeV. In each bin the Poisson probability is evaluated for the observed number of data events given the model prediction. The model prediction is the sum of the expected background and the expected signal yield. The expected signal yield is a function of the graviton mass m_G and the signal cross section times the branching ratio $\sigma \times B(G \rightarrow \gamma\gamma)$. Systematic uncertainties are incorporated as nuisance parameters with Gaussian priors; the computation of the likelihood function includes integration over the variation in each of these. The RS model results can be combined with the results from the dilepton channel [3] to obtain limits on $\sigma \times B(G \rightarrow \gamma\gamma/ee/\mu\mu)$. Relative branching ratios of $B(G \rightarrow ee)/B(G \rightarrow \mu\mu) = 1$ and $B(G \rightarrow \gamma\gamma)/B(G \rightarrow ee) = 2$ [48] are assumed for the purpose of this combination. Correlations between the systematic uncertainties for different channels are taken into account in the combination, as discussed in [11]. Specifically, the systematic uncertainty in the QCD dijet background is treated as fully correlated across the ee and $\gamma\gamma$ channels. The PDF and scale uncertainties are treated as correlated across all three channels, and affect the irreducible background in the $\gamma\gamma$ channel as well as the Drell–Yan background in the $ee/\mu\mu$ channels. The resulting limits are shown in figure 3. The limit can be interpreted in the plane $(m_G, k/\overline{M}_{\text{Pl}})$ using the theoretical dependence of the cross section on these parameters (figure 4). Alternatively, for a given value of $k/\overline{M}_{\text{Pl}}$, the limit can be translated into a limit on m_G . The limits on m_G are summarized in table 2. Using a constant K -factor of 1.75, the 95 % CL lower limit from the diphoton channel is 1.00 (2.06) TeV for $k/\overline{M}_{\text{Pl}} = 0.01$ (0.1), and the combined 95% CL lower limit is 1.03 (2.23) TeV for $k/\overline{M}_{\text{Pl}} = 0.01$ (0.1).

A counting experiment is performed to set limits on the ADD model. Specifically, the number of diphoton events is counted in a search region above a given threshold in $m_{\gamma\gamma}$. The mass threshold is chosen to optimize the expected limit on the difference in the diphoton cross section for $m_{\gamma\gamma} > 500$ GeV between the ADD model and the SM-only hypothesis. For the purpose of this optimization, a specific implementation of the ADD model and specific values of the parameters have to be chosen. For $M_5 = 2500$ GeV in the GRW convention, an optimal search region is obtained at $m_{\gamma\gamma} > 1217$ GeV. In the data, four events are observed in this search region, with a background expectation of 2.32 ± 0.37 events. The expected and observed 95% CL upper limits on the number of signal events above the SM background in the search region are given in table 3.

These limits on the event yield can be translated into limits on the parameter η_G of the ADD model using a prediction of the expected excess of events over the SM-only background as a

⁵ While the background is normalized to the data in the low-mass control region, the presence of a bump inside this region would still be visible. This motivates the choice of the lower limit of the search region.

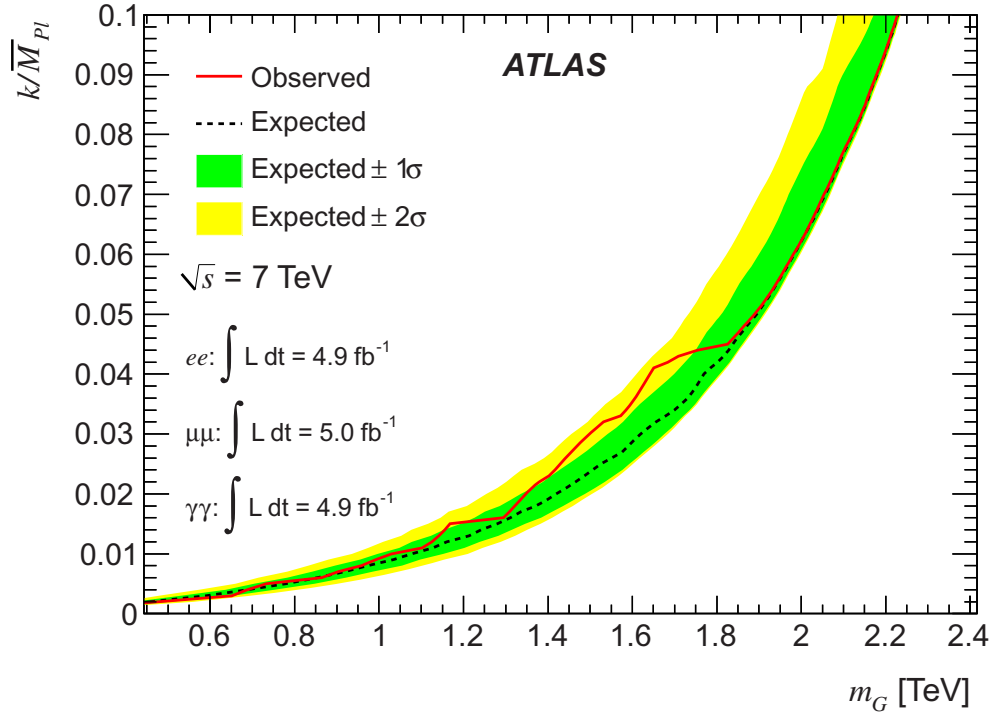


Figure 4. The RS results interpreted in the plane of $k/\overline{M}_{\text{Pl}}$ versus graviton mass. The region above the curve is excluded at 95% CL.

Table 2. The 95% CL lower limits on the mass (TeV) of the lightest RS graviton, for various values of $k/\overline{M}_{\text{Pl}}$. The results are shown for the diphoton channel alone and for the combination of the diphoton and dilepton channels, and also for both LO and NLO (K -factor = 1.75) theory cross-section calculations.

K -factor value	Channel(s) used	95% CL observed (expected) limit (TeV)			
		$k/\overline{M}_{\text{Pl}}$ value			
		0.01	0.03	0.05	0.1
1	$G \rightarrow \gamma\gamma$	0.87 (0.88)	1.31 (1.36)	1.49 (1.60)	1.91 (1.92)
	$G \rightarrow \gamma\gamma/ee/\mu\mu$	0.91 (0.95)	1.39 (1.48)	1.62 (1.75)	2.10 (2.10)
1.75	$G \rightarrow \gamma\gamma$	1.00 (0.98)	1.37 (1.49)	1.63 (1.73)	2.06 (2.05)
	$G \rightarrow \gamma\gamma/ee/\mu\mu$	1.03 (1.08)	1.50 (1.63)	1.89 (1.90)	2.23 (2.23)

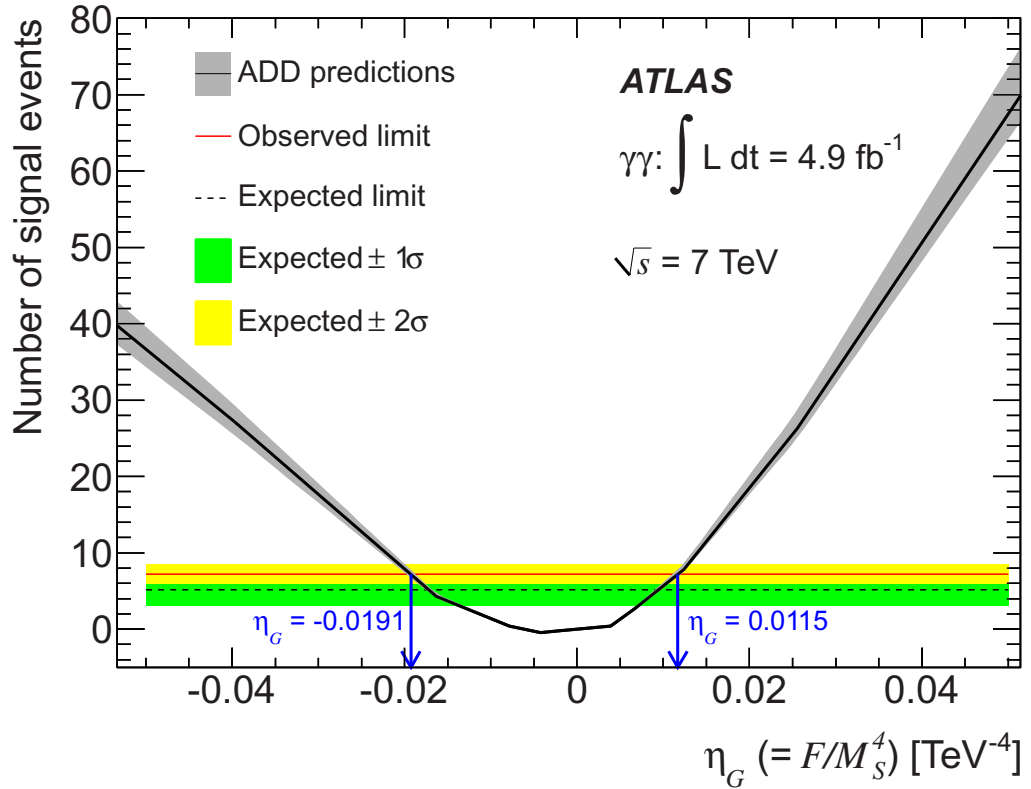
function of η_G . This translation is shown, for one specific implementation of the ADD model, in figure 5.

The limits⁶ for different ADD scenarios are summarized in table 4. Using a constant K -factor of 1.70, the 95% CL upper (lower) limit on η_G is 0.0085 (-0.0159) TeV^{-4} for constructive (destructive) interference.

⁶ The limit in the HLZ convention with $n = 2$ may appear weak compared to the corresponding limit reported in [12]. When adopting the same search region as in [12], namely $m_{\gamma\gamma} > 901$ GeV instead of $m_{\gamma\gamma} > 1217$ GeV, our HLZ, $n = 2$ limit for a K -factor=1 becomes $M_S = 3.57$ TeV, which is more stringent than the result obtained with our default search region.

Table 3. The expected and observed limits at 95% CL on the number of signal events in the search region at $m_{\gamma\gamma} > 1217$ GeV.

Expected limit					Observed limit
-2σ	-1σ	Mean	$+1\sigma$	$+2\sigma$	
3.08	3.08	5.18	5.96	8.53	7.21

**Figure 5.** The number of signal events as a function of η_G . The solid horizontal line corresponds to the observed limit, the dashed line to the expected limit and the bands to the $\pm 1\sigma$ and $\pm 2\sigma$ uncertainty on the expected limit. The black curve corresponds to MC predictions from various samples without applying the K -factor of 1.70. The band around it illustrates the theoretical uncertainties due to the PDFs expressed at 90% CL. The samples at positive (negative) η_G have been simulated using the GRW (Hewett) formalism. When the prediction is greater than the observed limit, the corresponding value of η_G is excluded.

8. Summary

A search for evidence of extra dimensions has been performed in the diphoton channel, based on the full 2011 dataset collected by the ATLAS detector at the LHC (4.9 fb^{-1} of proton–proton collisions at $\sqrt{s} = 7 \text{ TeV}$). In the ADD scenario, lower limits of between 2.52 and 3.92 TeV

Table 4. The observed 95% CL limits on the ADD model parameters η_G (TeV^{-4}) and M_S (TeV) for various ADD models.

K-factor value	ADD parameter	GRW	Hewett		HLZ					
			Neg.	Pos.	$n = 2$	$n = 3$	$n = 4$	$n = 5$	$n = 6$	$n = 7$
1	η_G	0.0115	-0.0191	0.0115			0.0115			
	M_S	3.05	2.40	2.73	3.11	3.63	3.05	2.76	2.57	2.43
1.70	η_G	0.0085	-0.0159	0.0085			0.0085			
	M_S	3.29	2.52	2.94	3.55	3.92	3.29	2.98	2.77	2.62

at 95% CL are set on the M_S scale, depending on the number of extra dimensions and the theoretical formalism used. The combination with the dilepton channel presented in [49] further tightened these limits to 2.6–4.2 TeV.

In the RS scenario, a lower limit of 1.00 (2.06) TeV at 95% CL is set on the mass of the lightest RS graviton, for RS couplings of $k/\overline{M}_{\text{Pl}} = 0.01$ (0.1). These new limits are a significant improvement over the previous best limit in the diphoton channel of 0.80 (1.85) TeV for $k/\overline{M}_{\text{Pl}} = 0.01$ (0.1) [11]. The combination with the latest ATLAS dilepton searches [3] yields an improvement by a factor of 2–3 in the cross-section limits compared to [11] and further tightens the RS graviton mass limits to 1.03 (2.23) TeV for $k/\overline{M}_{\text{Pl}} = 0.01$ (0.1).

Acknowledgments

We are grateful to the CERN for the very successful operation of the LHC, as well as the support staff from our institutions without whom ATLAS could not be operated efficiently. We acknowledge support from ANPCyT, Argentina; YerPhI, Armenia; ARC, Australia; BMWF and FWF, Austria; ANAS, Azerbaijan; SSTC, Belarus; CNPq and FAPESP, Brazil; NSERC, NRC and CFI, Canada; CERN; CONICYT, Chile; CAS, MOST and NSFC, China; COLCIENCIAS, Colombia; MSMT CR, MPO CR and VSC CR, Czech Republic; DNRF, DNSRC and Lundbeck Foundation, Denmark; EPLANET and ERC, the European Union; IN2P3-CNRS, CEA-DSM/IRFU, France; GNSF, Georgia; BMBF, DFG, HGF, MPG and AvH Foundation, Germany; GSRT, Greece; ISF, MINERVA, GIF, DIP and Benoziyo Center, Israel; INFN, Italy; MEXT and JSPS, Japan; CNRST, Morocco; FOM and NWO, Netherlands; BRF and RCN, Norway; MNiSW, Poland; GRICES and FCT, Portugal; MERYS (MECTS), Romania; MES of Russia and ROSATOM, Russian Federation; JINR; MSTQ, Serbia; MSSR, Slovakia; ARRS and MVZT, Slovenia; DST/NRF, South Africa; MICINN, Spain; SRC and Wallenberg Foundation, Sweden; SER, SNSF and Cantons of Bern and Geneva, Switzerland; NSC, Taiwan; TAEK, Turkey; STFC, the Royal Society and Leverhulme Trust, UK; and DOE and NSF, USA. Crucial computing support from all WLCG partners is gratefully acknowledged, in particular, from CERN and the ATLAS Tier-1 facilities at TRIUMF (Canada), NDGF (Denmark, Norway, Sweden), CC-IN2P3 (France), KIT/GridKA (Germany), INFN-CNAF (Italy), NL-T1 (the Netherlands), PIC (Spain), ASGC (Taiwan), RAL (UK) and BNL (USA) and the Tier-2 facilities worldwide.

The ATLAS Collaboration

G Aad⁴⁸, T Abajyan²¹, B Abbott¹¹¹, J Abdallah¹², S Abdel Khalek¹¹⁵, A A Abdelalim⁴⁹, O Abidinov¹¹, R Aben¹⁰⁵, B Abi¹¹², M Abolins⁸⁸, O S AbouZeid¹⁵⁸, H Abramowicz¹⁵³, H Abreu¹³⁶, B S Acharya^{164a,164b}, L Adamczyk³⁸, D L Adams²⁵, T N Addy⁵⁶, J Adelman¹⁷⁶, S Adomeit⁹⁸, P Adragna⁷⁵, T Adye¹²⁹, S Aefsky²³, J A Aguilar-Saavedra^{124b,179}, M Agustoni¹⁷, M Aharrouche⁸¹, S P Ahlen²², F Ahles⁴⁸, A Ahmad¹⁴⁸, M Ahsan⁴¹, G Aielli^{133a,133b}, T Akdogan^{19a}, T P A Åkesson⁷⁹, G Akimoto¹⁵⁵, A V Akimov⁹⁴, M S Alam², M A Alam⁷⁶, J Albert¹⁶⁹, S Albrand⁵⁵, M Aleksa³⁰, I N Aleksandrov⁶⁴, F Alessandria^{89a}, C Alexa^{26a}, G Alexander¹⁵³, G Alexandre⁴⁹, T Alexopoulos¹⁰, M Alhroob^{164a,164c}, M Aliev¹⁶, G Alimonti^{89a}, J Alison¹²⁰, B M M Allbrooke¹⁸, P P Allport⁷³, S E Allwood-Spiers⁵³, J Almond⁸², A Aloisio^{102a,102b}, R Alon¹⁷², A Alonso⁷⁹, F Alonso⁷⁰, A Altheimer³⁵, B Alvarez Gonzalez⁸⁸, M G Alviggi^{102a,102b}, K Amako⁶⁵, C Amelung²³, V V Ammosov^{128,218}, S P Amor Dos Santos^{124a}, A Amorim^{124a,180}, N Amram¹⁵³, C Anastopoulos³⁰, L S Ancu¹⁷, N Andari¹¹⁵, T Andeen³⁵, C F Anders^{58b}, G Anders^{58a}, K J Anderson³¹, A Andreazza^{89a,89b}, V Andrei^{58a}, M-L Andrieux⁵⁵, X S Anduaga⁷⁰, P Anger⁴⁴, A Angerami³⁵, F Anghinolfi³⁰, A Anisenkov¹⁰⁷, N Anjos^{124a}, A Annovi⁴⁷, A Antonaki⁹, M Antonelli⁴⁷, A Antonov⁹⁶, J Antos^{144b}, F Anulli^{132a}, M Aoki¹⁰¹, S Aoun⁸³, L Aperio Bella⁵, R Apolle^{118,181}, G Arabidze⁸⁸, I Aracena¹⁴³, Y Arai⁶⁵, A T H Arce⁴⁵, S Arfaoui¹⁴⁸, J-F Arguin¹⁵, E Arik^{19a,218}, M Arik^{19a}, A J Armbruster⁸⁷, O Arnaez⁸¹, V Arnal⁸⁰, C Arnault¹¹⁵, A Artamonov⁹⁵, G Artoni^{132a,132b}, D Arutinov²¹, S Asai¹⁵⁵, R Asfandiyarov¹⁷³, S Ask²⁸, B Åsman^{146a,146b}, L Asquith⁶, K Assamagan^{25,182}, A Astbury¹⁶⁹, M Atkinson¹⁶⁵, B Aubert⁵, E Auge¹¹⁵, K Augsten¹²⁷, M Aourousseau^{145a}, G Avolio¹⁶³, R Avramidou¹⁰, D Axen¹⁶⁸, G Azuelos^{93,183}, Y Azuma¹⁵⁵, M A Baak³⁰, G Baccaglioni^{89a}, C Bacci^{134a,134b}, A M Bach¹⁵, H Bachacou¹³⁶, K Bachas³⁰, M Backes⁴⁹, M Backhaus²¹, E Badescu^{26a}, P Bagnaia^{132a,132b}, S Bahinipati³, Y Bai^{33a}, D C Bailey¹⁵⁸, T Bain¹⁵⁸, J T Baines¹²⁹, O K Baker¹⁷⁶, M D Baker²⁵, S Baker⁷⁷, E Banas³⁹, P Banerjee⁹³, Sw Banerjee¹⁷³, D Banfi³⁰, A Bangert¹⁵⁰, V Bansal¹⁶⁹, H S Bansil¹⁸, L Barak¹⁷², S P Baranov⁹⁴, A Barbaro Galtieri¹⁵, T Barber⁴⁸, E L Barberio⁸⁶, D Barberis^{50a,50b}, M Barbero²¹, D Y Bardin⁶⁴, T Barillari⁹⁹, M Barisonzi¹⁷⁵, T Barklow¹⁴³, N Barlow²⁸, B M Barnett¹²⁹, R M Barnett¹⁵, A Baroncelli^{134a}, G Barone⁴⁹, A J Barr¹¹⁸, F Barreiro⁸⁰, J Barreiro Guimarães da Costa⁵⁷, P Barrillon¹¹⁵, R Bartoldus¹⁴³, A E Barton⁷¹, V Bartsch¹⁴⁹, A Basye¹⁶⁵, R L Bates⁵³, L Batkova^{144a}, J R Batley²⁸, A Battaglia¹⁷, M Battistin³⁰, F Bauer¹³⁶, H S Bawa^{143,184}, S Beale⁹⁸, T Beau⁷⁸, P H Beauchemin¹⁶¹, R Beccherle^{50a}, P Bechtel²¹, H P Beck¹⁷, K Becker¹⁷⁵, S Becker⁹⁸, M Beckingham¹³⁸, K H Becks¹⁷⁵, A J Beddall^{19c}, A Beddall^{19c}, S Bedikian¹⁷⁶, V A Bednyakov⁶⁴, C P Bee⁸³, L J Beemster¹⁰⁵, M Begel²⁵, S Behar Harpaz¹⁵², P K Behera⁶², M Beimforde⁹⁹, C Belanger-Champagne⁸⁵, P J Bell⁴⁹, W H Bell⁴⁹, G Bella¹⁵³, L Bellagamba^{20a}, F Bellina³⁰, M Bellomo³⁰, A Belloni⁵⁷, O Beloborodova^{107,185}, K Belotskiy⁹⁶, O Beltramello³⁰, O Benary¹⁵³, D Bencheikroun^{135a}, K Bendtz^{146a,146b}, N Benekos¹⁶⁵, Y Benhammou¹⁵³, E Benhar Nocchioli⁴⁹, J A Benitez Garcia^{159b}, D P Benjamin⁴⁵, M Benoit¹¹⁵, J R Bensinger²³, K Benslama¹³⁰, S Bentvelsen¹⁰⁵, D Berge³⁰, E Bergeaas Kuutmann⁴², N Berger⁵, F Berghaus¹⁶⁹, E Berglund¹⁰⁵, J Beringer¹⁵, P Bernat⁷⁷, R Bernhard⁴⁸, C Bernius²⁵, T Berry⁷⁶, C Bertella⁸³, A Bertin^{20a,20b}, F Bertolucci^{122a,122b}, M I Besana^{89a,89b}, G J Besjes¹⁰⁴, N Besson¹³⁶, S Bethke⁹⁹, W Bhimji⁴⁶, R M Bianchi³⁰, M Bianco^{72a,72b}, O Biebel⁹⁸, S P Bieniek⁷⁷, K Bierwagen⁵⁴, J Biesiada¹⁵, M Biglietti^{134a}, H Bilokon⁴⁷, M Bindi^{20a,20b}, S Binet¹¹⁵, A Bingul^{19c}, C Bini^{132a,132b}, C Biscarat¹⁷⁸, B Bittner⁹⁹, K M Black²², R E Blair⁶, J-B Blanchard¹³⁶, G Blanchot³⁰, T Blazek^{144a}, I Bloch⁴², C Blocker²³, J Blocki³⁹, A Blondel⁴⁹, W Blum⁸¹, U Blumenschein⁵⁴, G J Bobbink¹⁰⁵, V S Bobrovnikov¹⁰⁷, S S Bocchetta⁷⁹, A Bocci⁴⁵, C R Boddy¹¹⁸, M Boehler⁴⁸,

J Boek¹⁷⁵, T T Boek¹⁷⁵, N Boelaert³⁶, J A Bogaerts³⁰, A Bogdanchikov¹⁰⁷, A Bogouch^{90,218}, C Bohm^{146a}, J Bohm¹²⁵, V Boisvert⁷⁶, T Bold³⁸, V Boldea^{26a}, N M Bolnet¹³⁶, M Bomben⁷⁸, M Bona⁷⁵, M Boonekamp¹³⁶, S Bordoni⁷⁸, C Borer¹⁷, A Borisov¹²⁸, G Borissov⁷¹, I Borjanovic^{13a}, M Borri⁸², S Borroni⁸⁷, V Bortolotto^{134a,134b}, K Bos¹⁰⁵, D Boscherini^{20a}, M Bosman¹², H Boterenbrood¹⁰⁵, J Bouchami⁹³, J Boudreau¹²³, E V Bouhova-Thacker⁷¹, D Boumediene³⁴, C Bourdarios¹¹⁵, N Bousson⁸³, A Boveia³¹, J Boyd³⁰, I R Boyko⁶⁴, I Bozovic-Jelisavcic^{13b}, J Bracinik¹⁸, P Branchini^{134a}, G W Brandenburg⁵⁷, A Brandt⁸, G Brandt¹¹⁸, O Brandt⁵⁴, U Bratzler¹⁵⁶, B Brau⁸⁴, J E Brau¹¹⁴, H M Braun^{175,218}, S F Brazzale^{164a,164c}, B Brelrier¹⁵⁸, J Bremer³⁰, K Brendlinger¹²⁰, R Brenner¹⁶⁶, S Bressler¹⁷², D Britton⁵³, F M Brochu²⁸, I Brock²¹, R Brock⁸⁸, F Broggi^{89a}, C Bromberg⁸⁸, J Bronner⁹⁹, G Brooijmans³⁵, T Brooks⁷⁶, W K Brooks^{32b}, G Brown⁸², H Brown⁸, P A Bruckman de Renstrom³⁹, D Bruncko^{144b}, R Bruneliere⁴⁸, S Brunet⁶⁰, A Bruni^{20a}, G Bruni^{20a}, M Bruschi^{20a}, T Buanes¹⁴, Q Buat⁵⁵, F Bucci⁴⁹, J Buchanan¹¹⁸, P Buchholz¹⁴¹, R M Buckingham¹¹⁸, A G Buckley⁴⁶, S I Buda^{26a}, I A Budagov⁶⁴, B Budick¹⁰⁸, V Büscher⁸¹, L Bugge¹¹⁷, O Bulekov⁹⁶, A C Bundock⁷³, M Bunse⁴³, T Buran¹¹⁷, H Burckhart³⁰, S Burdin⁷³, T Burgess¹⁴, S Burke¹²⁹, E Busato³⁴, P Bussey⁵³, C P Buszello¹⁶⁶, B Butler¹⁴³, J M Butler²², C M Buttar⁵³, J M Butterworth⁷⁷, W Buttinger²⁸, M Byszewski³⁰, S Cabrera Urbán¹⁶⁷, D Caforio^{20a,20b}, O Cakir^{4a}, P Calafiura¹⁵, G Calderini⁷⁸, P Calfayan⁹⁸, R Calkins¹⁰⁶, L P Caloba^{24a}, R Caloi^{132a,132b}, D Calvet³⁴, S Calvet³⁴, R Camacho Toro³⁴, P Camarri^{133a,133b}, D Cameron¹¹⁷, L M Caminada¹⁵, R Caminal Armadans¹², S Campana³⁰, M Campanelli⁷⁷, V Canale^{102a,102b}, F Canelli³¹, A Canepa^{159a}, J Cantero⁸⁰, R Cantrill⁷⁶, L Capasso^{102a,102b}, MDM Capeans Garrido³⁰, I Caprini^{26a}, M Caprini^{26a}, D Capriotti⁹⁹, M Capua^{37a,37b}, R Caputo⁸¹, R Cardarelli^{133a}, T Carli³⁰, G Carlino^{102a}, L Carminati^{89a,89b}, B Caron⁸⁵, S Caron¹⁰⁴, E Carquin^{32b}, G D Carrillo-Montoya¹⁷³, A A Carter⁷⁵, J R Carter²⁸, J Carvalho^{124a,186}, D Casadei¹⁰⁸, M P Casado¹², M Cascella^{122a,122b}, C Caso^{50a,50b,218}, A M Castaneda Hernandez^{173,187}, E Castaneda-Miranda¹⁷³, V Castillo Gimenez¹⁶⁷, N F Castro^{124a}, G Cataldi^{72a}, P Catastini⁵⁷, A Catinaccio³⁰, J R Catmore³⁰, A Cattai³⁰, G Cattani^{133a,133b}, S Caughron⁸⁸, V Cavaliere¹⁶⁵, P Cavalleri⁷⁸, D Cavalli^{89a}, M Cavalli-Sforza¹², V Cavasinni^{122a,122b}, F Ceradini^{134a,134b}, A S Cerqueira^{24b}, A Cerri³⁰, L Cerrito⁷⁵, F Cerutti⁴⁷, S A Cetin^{19b}, A Chafaq^{135a}, D Chakraborty¹⁰⁶, I Chalupkova¹²⁶, K Chan³, P Chang¹⁶⁵, B Chapleau⁸⁵, J D Chapman²⁸, J W Chapman⁸⁷, E Chareyre⁷⁸, D G Charlton¹⁸, V Chavda⁸², C A Chavez Barajas³⁰, S Cheatham⁸⁵, S Chekanov⁶, S V Chekulaev^{159a}, G A Chelkov⁶⁴, M A Chelstowska¹⁰⁴, C Chen⁶³, H Chen²⁵, S Chen^{33c}, X Chen¹⁷³, Y Chen³⁵, A Cheplakov⁶⁴, R Cherkaoui El Moursli^{135e}, V Chernyatin²⁵, E Cheu⁷, S L Cheung¹⁵⁸, L Chevalier¹³⁶, G Chiefari^{102a,102b}, L Chikovani^{51a,218}, J T Childers³⁰, A Chilingarov⁷¹, G Chiodini^{72a}, A S Chisholm¹⁸, R T Chislett⁷⁷, A Chitan^{26a}, M V Chizhov⁶⁴, G Choudalakis³¹, S Chouridou¹³⁷, I A Christidi⁷⁷, A Christov⁴⁸, D Chromek-Burckhart³⁰, M L Chu¹⁵¹, J Chudoba¹²⁵, G Ciapetti^{132a,132b}, A K Ciftci^{4a}, R Ciftci^{4a}, D Cinca³⁴, V Cindro⁷⁴, C Ciocca^{20a,20b}, A Ciocio¹⁵, M Cirilli⁸⁷, P Cirkovic^{13b}, Z H Citron¹⁷², M Citterio^{89a}, M Ciubancan^{26a}, A Clark⁴⁹, P J Clark⁴⁶, R N Clarke¹⁵, W Cleland¹²³, J C Clemens⁸³, B Clement⁵⁵, C Clement^{146a,146b}, Y Coadou⁸³, M Cobal^{164a,164c}, A Cocco¹³⁸, J Cochran⁶³, L Coffey²³, J G Cogan¹⁴³, J Coggeshall¹⁶⁵, E Cogneras¹⁷⁸, J Colas⁵, S Cole¹⁰⁶, A P Colijn¹⁰⁵, N J Collins¹⁸, C Collins-Tooth⁵³, J Collot⁵⁵, T Colombo^{119a,119b}, G Colon⁸⁴, P Conde Muiño^{124a}, E Coniavitis¹¹⁸, M C Conidi¹², S M Consonni^{89a,89b}, V Consorti⁴⁸, S Constantinescu^{26a}, C Conta^{119a,119b}, G Conti⁵⁷, F Conventi^{102a,188}, M Cooke¹⁵, B D Cooper⁷⁷, A M Cooper-Sarkar¹¹⁸, K Copic¹⁵, T Cornelissen¹⁷⁵, M Corradi^{20a}, F Corriveau^{85,189}, A Cortes-Gonzalez¹⁶⁵, G Cortiana⁹⁹, G Costa^{89a}, M J Costa¹⁶⁷, D Costanzo¹³⁹, D Côté³⁰, L Courneyea¹⁶⁹, G Cowan⁷⁶,

C Cowden²⁸, B E Cox⁸², K Cranmer¹⁰⁸, F Crescioli⁷⁸, M Cristinziani²¹, G Crosetti^{37a,37b}, S Crépé-Renaudin⁵⁵, C-M Cuciuc^{26a}, C Cuenca Almenar¹⁷⁶, T Cuhadar Donszelmann¹³⁹, M Curatolo⁴⁷, C J Curtis¹⁸, C Cuthbert¹⁵⁰, P Cwetanski⁶⁰, H Czirr¹⁴¹, P Czodrowski⁴⁴, Z Czyczula¹⁷⁶, S D'Auria⁵³, M D'Onofrio⁷³, A D'Orazio^{132a,132b}, M J Da Cunha Sargedas De Sousa^{124a}, C Da Via⁸², W Dabrowski³⁸, A Dafinca¹¹⁸, T Dai⁸⁷, C Dallapiccola⁸⁴, M Dam³⁶, M Dameri^{50a,50b}, D S Damiani¹³⁷, H O Danielsson³⁰, V Dao⁴⁹, G Darbo^{50a}, G L Darlea^{26b}, J A Dassoulas⁴², W Davey²¹, T Davidek¹²⁶, N Davidson⁸⁶, R Davidson⁷¹, E Davies^{118,181}, M Davies⁹³, O Davignon⁷⁸, A R Davison⁷⁷, Y Davygora^{58a}, E Dawe¹⁴², I Dawson¹³⁹, R K Daya-Ishmukhametova²³, K De⁸, R de Asmundis^{102a}, S DeCastro^{20a,20b}, S De Cecco⁷⁸, J de Graat⁹⁸, N De Groot¹⁰⁴, P de Jong¹⁰⁵, C De La Taille¹¹⁵, H De la Torre⁸⁰, F De Lorenzi⁶³, L de Mora⁷¹, L De Nooij¹⁰⁵, D De Pedis^{132a}, A De Salvo^{132a}, U De Sanctis^{164a,164c}, A De Santo¹⁴⁹, J B De Vivie De Regie¹¹⁵, G De Zorzi^{132a,132b}, W J Dearnaley⁷¹, R Debbe²⁵, C Debenedetti⁴⁶, B Dechenaux⁵⁵, D V Dedovich⁶⁴, J Degenhardt¹²⁰, C Del Papa^{164a,164c}, J Del Peso⁸⁰, T Del Prete^{122a,122b}, T Delemontex⁵⁵, M Deliyergiyev⁷⁴, A Dell'Acqua³⁰, L Dell'Asta²², M Della Pietra^{102a,188}, D della Volpe^{102a,102b}, M Delmastro⁵, P A Delsart⁵⁵, C Deluca¹⁰⁵, S Demers¹⁷⁶, M Demichev⁶⁴, B Demirköz^{12,190}, J Deng¹⁶³, S P Denisov¹²⁸, D Derendarz³⁹, J E Derkaoui^{135d}, F Derue⁷⁸, P Dervan⁷³, K Desch²¹, E Devetak¹⁴⁸, P O Deviveiros¹⁰⁵, A Dewhurst¹²⁹, B DeWilde¹⁴⁸, S Dhaliwal¹⁵⁸, R Dhullipudi^{25,191}, A Di Ciaccio^{133a,133b}, L Di Ciaccio⁵, A Di Girolamo³⁰, B Di Girolamo³⁰, S Di Luise^{134a,134b}, A Di Mattia¹⁷³, B Di Micco³⁰, R Di Nardo⁴⁷, A Di Simone^{133a,133b}, R Di Sipio^{20a,20b}, M A Diaz^{32a}, E B Diehl⁸⁷, J Dietrich⁴², T A Dietzsch^{58a}, S Diglio⁸⁶, K Dindar Yagci⁴⁰, J Dingfelder²¹, F Dinut^{26a}, C Dionisi^{132a,132b}, P Dita^{26a}, S Dita^{26a}, F Dittus³⁰, F Djama⁸³, T Djobava^{51b}, M A B do Vale^{24c}, A Do Valle Wemans^{124a,192}, T K O Doan⁵, M Dobbs⁸⁵, R Dobinson^{30,218}, D Dobos³⁰, E Dobson^{30,193}, J Dodd³⁵, C Doglioni⁴⁹, T Doherty⁵³, Y Doi^{65,218}, J Dolejsi¹²⁶, I Dolenc⁷⁴, Z Dolezal¹²⁶, B A Dolgoshein^{96,218}, T Dohmae¹⁵⁵, M Donadelli^{24d}, J Donini³⁴, J Dopke³⁰, A Doria^{102a}, A DosAnjos¹⁷³, A Dotti^{122a,122b}, M T Dova⁷⁰, A D Doxiadis¹⁰⁵, A T Doyle⁵³, N Dressnandt¹²⁰, M Dris¹⁰, J Dubbert⁹⁹, S Dube¹⁵, E Duchovni¹⁷², G Duckeck⁹⁸, D Duda¹⁷⁵, A Dudarev³⁰, F Dudziak⁶³, M Dührssen³⁰, I P Duerdoth⁸², L Duflot¹¹⁵, M-A Dufour⁸⁵, L Duguid⁷⁶, M Dunford³⁰, H Duran Yildiz^{4a}, R Duxfield¹³⁹, M Dwuznik³⁸, F Dydak³⁰, M Düren⁵², W L Ebenstein⁴⁵, J Ebke⁹⁸, S Eckweiler⁸¹, K Edmonds⁸¹, W Edson², C A Edwards⁷⁶, N C Edwards⁵³, W Ehrenfeld⁴², T Eifert¹⁴³, G Eigen¹⁴, K Einsweiler¹⁵, E Eisenhandler⁷⁵, T Ekelof¹⁶⁶, M El Kacimi^{135c}, M Ellert¹⁶⁶, S Elles⁵, F Ellinghaus⁸¹, K Ellis⁷⁵, N Ellis³⁰, J Elmsheuser⁹⁸, M Elsing³⁰, D Emeliyanov¹²⁹, R Engelmann¹⁴⁸, A Engl⁹⁸, B Epp⁶¹, J Erdmann⁵⁴, A Ereditato¹⁷, D Eriksson^{146a}, J Ernst², M Ernst²⁵, J Ernwein¹³⁶, D Errede¹⁶⁵, S Errede¹⁶⁵, E Ertel⁸¹, M Escalier¹¹⁵, H Esch⁴³, C Escobar¹²³, X Espinal Curull¹², B Esposito⁴⁷, F Etienne⁸³, A I Etiennev¹³⁶, E Etzion¹⁵³, D Evangelakou⁵⁴, H Evans⁶⁰, L Fabbri^{20a,20b}, C Fabre³⁰, R M Fakhrutdinov¹²⁸, S Falciano^{132a}, Y Fang¹⁷³, M Fanti^{89a,89b}, A Farbin⁸, A Farilla^{134a}, J Farley¹⁴⁸, T Farooque¹⁵⁸, S Farrell¹⁶³, S M Farrington¹⁷⁰, P Farthouat³⁰, F Fassi¹⁶⁷, P Fassnacht³⁰, D Fassouliotis⁹, B Fatholahzadeh¹⁵⁸, A Favareto^{89a,89b}, L Fayard¹¹⁵, S Fazio^{37a,37b}, R Febbraro³⁴, P Federic^{144a}, O L Fedin¹²¹, W Fedorko⁸⁸, M Fehling-Kaschek⁴⁸, L Feligioni⁸³, D Fellmann⁶, C Feng^{33d}, E J Feng⁶, A B Fenyuk¹²⁸, J Ferencei^{144b}, W Fernando⁶, S Ferrag⁵³, J Ferrando⁵³, V Ferrara⁴², A Ferrari¹⁶⁶, P Ferrari¹⁰⁵, R Ferrari^{119a}, D E Ferreira de Lima⁵³, A Ferrer¹⁶⁷, D Ferrere⁴⁹, C Ferretti⁸⁷, A Ferretto Parodi^{50a,50b}, M Fiascaris³¹, F Fiedler⁸¹, A Filipčič⁷⁴, F Filthaut¹⁰⁴, M Fincke-Keeler¹⁶⁹, M C N Fiolhais^{124a,186}, L Fiorini¹⁶⁷, A Firan⁴⁰, G Fischer⁴², M J Fisher¹⁰⁹, M Flechl¹⁴⁸, I Fleck¹⁴¹, J Fleckner⁸¹, P Fleischmann¹⁷⁴, S Fleischmann¹⁷⁵, T Flick¹⁷⁵, A Floderus⁷⁹, L R Flores Castillo¹⁷³, M J Flowerdew⁹⁹,

T Fonseca Martin¹⁷, A Formica¹³⁶, A Forti⁸², D Fortin^{159a}, D Fournier¹¹⁵, A J Fowler⁴⁵, H Fox⁷¹, P Francavilla¹², M Franchini^{20a,20b}, S Franchino^{119a,119b}, D Francis³⁰, T Frank¹⁷², S Franz³⁰, M Fraternali^{119a,119b}, S Fratina¹²⁰, S T French²⁸, C Friedrich⁴², F Friedrich⁴⁴, R Froeschl³⁰, D Froidevaux³⁰, J A Frost²⁸, C Fukunaga¹⁵⁶, E Fullana Torregrosa³⁰, B G Fulsom¹⁴³, J Fuster¹⁶⁷, C Gabaldon³⁰, O Gabizon¹⁷², T Gadfort²⁵, S Gadomski⁴⁹, G Gagliardi^{50a,50b}, P Gagnon⁶⁰, C Galea⁹⁸, B Galhardo^{124a}, E J Gallas¹¹⁸, V Gallo¹⁷, B J Gallop¹²⁹, P Gallus¹²⁵, K K Gan¹⁰⁹, Y S Gao^{143,184}, A Gaponenko¹⁵, F Garberson¹⁷⁶, M Garcia-Sciveres¹⁵, C García¹⁶⁷, J E García Navarro¹⁶⁷, R W Gardner³¹, N Garelli³⁰, H Garitaonandia¹⁰⁵, V Garonne³⁰, C Gatti⁴⁷, G Gaudio^{119a}, B Gaur¹⁴¹, L Gauthier¹³⁶, P Gauzzi^{132a,132b}, I L Gavrilenko⁹⁴, C Gay¹⁶⁸, G Gaycken²¹, E N Gazis¹⁰, P Ge^{33d}, Z Gecse¹⁶⁸, C N P Gee¹²⁹, D A A Geerts¹⁰⁵, Ch Geich-Gimbel²¹, K Gellerstedt^{146a,146b}, C Gemme^{50a}, A Gemmell⁵³, M H Genest⁵⁵, S Gentile^{132a,132b}, M George⁵⁴, S George⁷⁶, P Gerlach¹⁷⁵, A Gershon¹⁵³, C Geweniger^{58a}, H Ghazlane^{135b}, N Ghodbane³⁴, B Giacobbe^{20a}, S Giagu^{132a,132b}, V Giakoumopoulou⁹, V Giangiobbe¹², F Gianotti³⁰, B Gibbard²⁵, A Gibson¹⁵⁸, S M Gibson³⁰, M Gilchriese¹⁵, D Gillberg²⁹, A R Gillman¹²⁹, D M Gingrich^{3,183}, J Ginzburg¹⁵³, N Giokaris⁹, M P Giordani^{164c}, R Giordano^{102a,102b}, F M Giorgi¹⁶, P Giovannini⁹⁹, P F Giraud¹³⁶, D Giugni^{89a}, M Giunta⁹³, P Giusti^{20a}, B K Gjelsten¹¹⁷, L K Gladilin⁹⁷, C Glasman⁸⁰, J Glatzer⁴⁸, A Glazov⁴², K W Glitza¹⁷⁵, G L Glonti⁶⁴, J R Goddard⁷⁵, J Godfrey¹⁴², J Godlewski³⁰, M Goebel⁴², T Göpfert⁴⁴, C Goeringer⁸¹, C Gössling⁴³, S Goldfarb⁸⁷, T Golling¹⁷⁶, A Gomes^{124a,180}, L S Gomez Fajardo⁴², R Gonçalo⁷⁶, J Goncalves Pinto Firmino Da Costa⁴², L Gonella²¹, S González de la Hoz¹⁶⁷, G Gonzalez Parra¹², M L Gonzalez Silva²⁷, S Gonzalez-Sevilla⁴⁹, J J Goodson¹⁴⁸, L Goossens³⁰, P A Gorbounov⁹⁵, H A Gordon²⁵, I Gorelov¹⁰³, G Gorfine¹⁷⁵, B Gorini³⁰, E Gorini^{72a,72b}, A Gorišek⁷⁴, E Gornicki³⁹, B Gosdzik⁴², A T Goshaw⁶, M Gosselink¹⁰⁵, M I Gostkin⁶⁴, I Gough Eschrich¹⁶³, M Goughri^{135a}, D Goujdami^{135c}, M P Goulette⁴⁹, A G Goussiou¹³⁸, C Goy⁵, S Gozpinar²³, I Grabowska-Bold³⁸, P Grafström^{20a,20b}, K-J Grahn⁴², F Grancagnolo^{72a}, S Grancagnolo¹⁶, V Grassi¹⁴⁸, V Gratchev¹²¹, N Grau³⁵, H M Gray³⁰, J A Gray¹⁴⁸, E Graziani^{134a}, O G Grebenyuk¹²¹, T Greenshaw⁷³, Z D Greenwood^{25,191}, K Gregersen³⁶, I M Gregor⁴², P Grenier¹⁴³, J Griffiths⁸, N Grigalashvili⁶⁴, A A Grillo¹³⁷, S Grinstein¹², Ph Gris³⁴, Y V Grishkevich⁹⁷, J-F Grivaz¹¹⁵, E Gross¹⁷², J Grosse-Knetter⁵⁴, J Groth-Jensen¹⁷², K Grybel¹⁴¹, D Guest¹⁷⁶, C Guicheney³⁴, S Guindon⁵⁴, U Gul⁵³, H Guler^{85,194}, J Gunther¹²⁵, B Guo¹⁵⁸, J Guo³⁵, P Gutierrez¹¹¹, N Guttman¹⁵³, O Gutzwiller¹⁷³, C Guyot¹³⁶, C Gwenlan¹¹⁸, C B Gwilliam⁷³, A Haas¹⁴³, S Haas³⁰, C Haber¹⁵, H K Hadavand⁴⁰, D R Hadley¹⁸, P Haefner²¹, F Hahn³⁰, S Haider³⁰, Z Hajduk³⁹, H Hakobyan¹⁷⁷, D Hall¹¹⁸, J Haller⁵⁴, K Hamacher¹⁷⁵, P Hamal¹¹³, K Hamano⁸⁶, M Hamer⁵⁴, A Hamilton^{145b,195}, S Hamilton¹⁶¹, L Han^{33b}, K Hanagaki¹¹⁶, K Hanawa¹⁶⁰, M Hance¹⁵, C Handel⁸¹, P Hanke^{58a}, J R Hansen³⁶, J B Hansen³⁶, J D Hansen³⁶, P H Hansen³⁶, P Hansson¹⁴³, K Hara¹⁶⁰, G A Hare¹³⁷, T Harenberg¹⁷⁵, S Harkusha⁹⁰, D Harper⁸⁷, R D Harrington⁴⁶, O M Harris¹³⁸, J Hartert⁴⁸, F Hartjes¹⁰⁵, T Haruyama⁶⁵, A Harvey⁵⁶, S Hasegawa¹⁰¹, Y Hasegawa¹⁴⁰, S Hassani¹³⁶, S Haug¹⁷, M Hauschild³⁰, R Hauser⁸⁸, M Havranek²¹, C M Hawkes¹⁸, R J Hawkings³⁰, A D Hawkins⁷⁹, T Hayakawa⁶⁶, T Hayashi¹⁶⁰, D Hayden⁷⁶, C P Hays¹¹⁸, H S Hayward⁷³, S J Haywood¹²⁹, S J Head¹⁸, V Hedberg⁷⁹, L Heelan⁸, S Heim⁸⁸, B Heinemann¹⁵, S Heisterkamp³⁶, L Helary²², C Heller⁹⁸, M Heller³⁰, S Hellman^{146a,146b}, D Hellmich²¹, C Helsens¹², R C W Henderson⁷¹, M Henke^{58a}, A Henrichs⁵⁴, A M Henriques Correia³⁰, S Henrot-Versille¹¹⁵, C Hensel⁵⁴, T Henß¹⁷⁵, C M Hernandez⁸, Y Hernández Jiménez¹⁶⁷, R Herrberg¹⁶, G Herten⁴⁸, R Hertenberger⁹⁸, L Hervas³⁰, G G Hesketh⁷⁷, N P Hessey¹⁰⁵, E Higón-Rodriguez¹⁶⁷, J C Hill²⁸, K H Hiller⁴²,

S Hillert²¹, S J Hillier¹⁸, I Hinchliffe¹⁵, E Hines¹²⁰, M Hirose¹¹⁶, F Hirsch⁴³, D Hirschbuehl¹⁷⁵, J Hobbs¹⁴⁸, N Hod¹⁵³, M C Hodgkinson¹³⁹, P Hodgson¹³⁹, A Hoecker³⁰, M R Hoefkamp¹⁰³, J Hoffman⁴⁰, D Hoffmann⁸³, M Hohlfeld⁸¹, M Holder¹⁴¹, S O Holmgren^{146a}, T Holy¹²⁷, J L Holzbauer⁸⁸, T M Hong¹²⁰, L Hooft van Huysduynen¹⁰⁸, S Horner⁴⁸, J-Y Hostachy⁵⁵, S Hou¹⁵¹, A Hoummada^{135a}, J Howard¹¹⁸, J Howarth⁸², I Hristova¹⁶, J Hrivnac¹¹⁵, T Hryn'ova⁵, P J Hsu⁸¹, S-C Hsu¹⁵, D Hu³⁵, Z Hubacek¹²⁷, F Hubaut⁸³, F Huegging²¹, A Huettmann⁴², T B Huffman¹¹⁸, E W Hughes³⁵, G Hughes⁷¹, M Huhtinen³⁰, M Hurwitz¹⁵, U Husemann⁴², N Huseynov^{64,196}, J Huston⁸⁸, J Huth⁵⁷, G Iacobucci⁴⁹, G Iakovidis¹⁰, M Ibbotson⁸², I Ibragimov¹⁴¹, L Iconomidou-Fayard¹¹⁵, J Idarraga¹¹⁵, P Iengo^{102a}, O Igonkina¹⁰⁵, Y Ikegami⁶⁵, M Ikeno⁶⁵, D Iliadis¹⁵⁴, N Ilic¹⁵⁸, T Ince²¹, J Inigo-Golfin³⁰, P Ioannou⁹, M Iodice^{134a}, K Iordanidou⁹, V Ippolito^{132a,132b}, A Irls Quiles¹⁶⁷, C Isaksson¹⁶⁶, M Ishino⁶⁷, M Ishitsuka¹⁵⁷, R Ishmukhametov⁴⁰, C Issever¹¹⁸, S Istin^{19a}, A V Ivashin¹²⁸, W Iwanski³⁹, H Iwasaki⁶⁵, J M Izen⁴¹, V Izzo^{102a}, B Jackson¹²⁰, J N Jackson⁷³, P Jackson¹, M R Jaekel³⁰, V Jain⁶⁰, K Jakobs⁴⁸, S Jakobsen³⁶, T Jakoubek¹²⁵, J Jakubek¹²⁷, D O Jamin¹⁵¹, D K Jana¹¹¹, E Jansen⁷⁷, H Jansen³⁰, A Jantsch⁹⁹, M Janus⁴⁸, R C Jared¹⁷³, G Jarlskog⁷⁹, L Jeanty⁵⁷, I Jen-La Plante³¹, D Jennens⁸⁶, P Jenni³⁰, A E Loevschall-Jensen³⁶, P Jež³⁶, S Jézéquel⁵, M K Jha^{20a}, H Ji¹⁷³, W Ji⁸¹, J Jia¹⁴⁸, Y Jiang^{33b}, M Jimenez Belenguer⁴², S Jin^{33a}, O Jinnouchi¹⁵⁷, M D Joergensen³⁶, D Joffe⁴⁰, M Johansen^{146a,146b}, K E Johansson^{146a}, P Johansson¹³⁹, S Johnert⁴², K A Johns⁷, K Jon-And^{146a,146b}, G Jones¹⁷⁰, R W L Jones⁷¹, T J Jones⁷³, C Joram³⁰, P M Jorge^{124a}, K D Joshi⁸², J Jovicevic¹⁴⁷, T Jovin^{13b}, X Ju¹⁷³, C A Jung⁴³, R M Jungst³⁰, V Juranek¹²⁵, P Jussel⁶¹, A Juste Rozas¹², S Kabana¹⁷, M Kaci¹⁶⁷, A Kaczmarzka³⁹, P Kadlecik³⁶, M Kado¹¹⁵, H Kagan¹⁰⁹, M Kagan⁵⁷, E Kajomovitz¹⁵², S Kalinin¹⁷⁵, L V Kalinovskaya⁶⁴, S Kama⁴⁰, N Kanaya¹⁵⁵, M Kaneda³⁰, S Kaneti²⁸, T Kanno¹⁵⁷, V A Kantserov⁹⁶, J Kanzaki⁶⁵, B Kaplan¹⁰⁸, A Kapliy³¹, J Kaplon³⁰, D Kar⁵³, M Karagounis²¹, K Karakostas¹⁰, M Karnevskiy⁴², V Kartvelishvili⁷¹, A N Karyukhin¹²⁸, L Kashif¹⁷³, G Kasieczka^{58b}, R D Kass¹⁰⁹, A Kastanas¹⁴, M Kataoka⁵, Y Kataoka¹⁵⁵, E Katsoufis¹⁰, J Katzy⁴², V Kaushik⁷, K Kawagoe⁶⁹, T Kawamoto¹⁵⁵, G Kawamura⁸¹, M S Kayl¹⁰⁵, S Kazama¹⁵⁵, V F Kazanin¹⁰⁷, M Y Kazarinov⁶⁴, R Keeler¹⁶⁹, P T Keener¹²⁰, R Kehoe⁴⁰, M Keil⁵⁴, G D Kekelidze⁶⁴, J S Keller¹³⁸, M Kenyon⁵³, O Kepka¹²⁵, N Kerschen³⁰, B P Kerševan⁷⁴, S Kersten¹⁷⁵, K Kessoku¹⁵⁵, J Keung¹⁵⁸, F Khalil-zada¹¹, H Khandanyan^{146a,146b}, A Khanov¹¹², D Kharchenko⁶⁴, A Khodinov⁹⁶, A Khomich^{58a}, T J Khoo²⁸, G Khoraiuli²¹, A Khoroshilov¹⁷⁵, V Khovanskiy⁹⁵, E Khramov⁶⁴, J Khubua^{51b}, H Kim^{146a,146b}, S H Kim¹⁶⁰, N Kimura¹⁷¹, O Kind¹⁶, B T King⁷³, M King⁶⁶, R S B King¹¹⁸, J Kirk¹²⁹, A E Kiryunin⁹⁹, T Kishimoto⁶⁶, D Kisielewska³⁸, T Kitamura⁶⁶, T Kittelmann¹²³, K Kiuchi¹⁶⁰, E Kladiva^{144b}, M Klein⁷³, U Klein⁷³, K Kleinknecht⁸¹, M Klemetti⁸⁵, A Klier¹⁷², P Klimek^{146a,146b}, A Klimentov²⁵, R Klingenberg⁴³, J A Klinger⁸², E B Klinkby³⁶, T Klioutchnikova³⁰, P F Klok¹⁰⁴, S Klous¹⁰⁵, E-E Kluge^{58a}, T Kluge⁷³, P Kluit¹⁰⁵, S Kluth⁹⁹, N S Knecht¹⁵⁸, E Kneringer⁶¹, E B F G Knoops⁸³, A Knue⁵⁴, B R Ko⁴⁵, T Kobayashi¹⁵⁵, M Kobel⁴⁴, M Kocian¹⁴³, P Kodys¹²⁶, K Köneke³⁰, A C König¹⁰⁴, S Koenig⁸¹, L Köpke⁸¹, F Koetsveld¹⁰⁴, P Koevesarki²¹, T Koffas²⁹, E Koffeman¹⁰⁵, L A Kogan¹¹⁸, S Kohlmann¹⁷⁵, F Kohn⁵⁴, Z Kohout¹²⁷, T Kohriki⁶⁵, T Koi¹⁴³, G M Kolachev^{107,218}, H Kolanoski¹⁶, V Kolesnikov⁶⁴, I Koletsou^{89a}, J Koll⁸⁸, A A Komar⁹⁴, Y Komori¹⁵⁵, T Kondo⁶⁵, T Kono^{42,197}, A I Kononov⁴⁸, R Konoplich^{108,198}, N Konstantinidis⁷⁷, S Koperny³⁸, K Korcyl³⁹, K Kordas¹⁵⁴, A Korn¹¹⁸, A Korol¹⁰⁷, I Korolkov¹², E V Korolkova¹³⁹, V A Korotkov¹²⁸, O Kortner⁹⁹, S Kortner⁹⁹, V V Kostyukhin²¹, S Kotov⁹⁹, V M Kotov⁶⁴, A Kotwal⁴⁵, C Kourkoumelis⁹, V Kouskoura¹⁵⁴, A Koutsman^{159a}, R Kowalewski¹⁶⁹, T Z Kowalski³⁸, W Kozanecki¹³⁶, A S Kozhin¹²⁸, V Kral¹²⁷, V A Kramarenko⁹⁷, G Kramberger⁷⁴,

M W Krasny⁷⁸, A Krasznahorkay¹⁰⁸, J K Kraus²¹, S Kreiss¹⁰⁸, F Krejci¹²⁷, J Kretzschmar⁷³, N Krieger⁵⁴, P Krieger¹⁵⁸, K Kroeninger⁵⁴, H Kroha⁹⁹, J Kroll¹²⁰, J Kroseberg²¹, J Krstic^{13a}, U Kruchonak⁶⁴, H Krüger²¹, T Kruker¹⁷, N Krumnack⁶³, Z V Krumshteyn⁶⁴, T Kubota⁸⁶, S Kuday^{4a}, S Kuehn⁴⁸, A Kugel^{58c}, T Kuhl⁴², D Kuhn⁶¹, V Kukhtin⁶⁴, Y Kulchitsky⁹⁰, S Kuleshov^{32b}, C Kummer⁹⁸, M Kuna⁷⁸, J Kunkle¹²⁰, A Kupco¹²⁵, H Kurashige⁶⁶, M Kurata¹⁶⁰, Y A Kurochkin⁹⁰, V Kus¹²⁵, E S Kuwertz¹⁴⁷, M Kuze¹⁵⁷, J Kvita¹⁴², R Kwee¹⁶, A La Rosa⁴⁹, L La Rotonda^{37a,37b}, L Labarga⁸⁰, J Labbe⁵, S Lablak^{135a}, C Lacasta¹⁶⁷, F Lacava^{132a,132b}, H Lacker¹⁶, D Lacour⁷⁸, V R Lacuesta¹⁶⁷, E Ladygin⁶⁴, R Lafaye⁵, B Laforge⁷⁸, T Lagouri¹⁷⁶, S Lai⁴⁸, E Laisne⁵⁵, M Lamanna³⁰, L Lambourne⁷⁷, C L Lampen⁷, W Lampl⁷, E Lancon¹³⁶, U Landgraf⁴⁸, M P J Landon⁷⁵, J L Lane⁸², V S Lang^{58a}, C Lange⁴², A J Lankford¹⁶³, F Lanni²⁵, K Lantzsch¹⁷⁵, A Lanza^{119a}, S Laplace⁷⁸, C Lapoire²¹, J F Laporte¹³⁶, T Lari^{89a}, A Larner¹¹⁸, M Lassnig³⁰, P Laurelli⁴⁷, V Lavorini^{37a,37b}, W Lavrijsen¹⁵, P Laycock⁷³, O Le Dortz⁷⁸, E Le Guirriec⁸³, E Le Menedeu¹², T LeCompte⁶, F Ledroit-Guillon⁵⁵, H Lee¹⁰⁵, J S H Lee¹¹⁶, S C Lee¹⁵¹, L Lee¹⁷⁶, M Lefebvre¹⁶⁹, M Legendre¹³⁶, F Legger⁹⁸, C Leggett¹⁵, M Lehmacher²¹, G Lehmann Miotto³⁰, M A L Leite^{24d}, R Leitner¹²⁶, D Lellouch¹⁷², B Lemmer⁵⁴, V Lendermann^{58a}, K J C Leney^{145b}, T Lenz¹⁰⁵, G Lenzen¹⁷⁵, B Lenzi³⁰, K Leonhardt⁴⁴, S Leontsinis¹⁰, F Lepold^{58a}, C Leroy⁹³, J-R Lessard¹⁶⁹, C G Lester²⁸, C M Lester¹²⁰, J Levêque⁵, D Levin⁸⁷, L J Levinson¹⁷², A Lewis¹¹⁸, G H Lewis¹⁰⁸, A M Leyko²¹, M Leyton¹⁶, B Li⁸³, H Li^{173,199}, S Li^{33b,200}, X Li⁸⁷, Z Liang^{118,201}, H Liao³⁴, B Liberti^{133a}, P Lichard³⁰, M Lichtnecker⁹⁸, K Lie¹⁶⁵, W Liebig¹⁴, C Limbach²¹, A Limosani⁸⁶, M Limper⁶², S C Lin^{151,202}, F Linde¹⁰⁵, J T Linnemann⁸⁸, E Lipeles¹²⁰, A Lipniacka¹⁴, T M Liss¹⁶⁵, D Lissauer²⁵, A Lister⁴⁹, A M Litke¹³⁷, C Liu²⁹, D Liu¹⁵¹, H Liu⁸⁷, J B Liu⁸⁷, L Liu⁸⁷, M Liu^{33b}, Y Liu^{33b}, M Livan^{119a,119b}, S S A Livermore¹¹⁸, A Lleres⁵⁵, J Llorente Merino⁸⁰, S L Lloyd⁷⁵, E Lobodzinska⁴², P Loch⁷, W S Lockman¹³⁷, T Loddenkoetter²¹, F K Loebinger⁸², A Loginov¹⁷⁶, C W Loh¹⁶⁸, T Lohse¹⁶, K Lohwasser⁴⁸, M Lokajicek¹²⁵, V P Lombardo⁵, R E Long⁷¹, L Lopes^{124a}, D Lopez Mateos⁵⁷, J Lorenz⁹⁸, N Lorenzo Martinez¹¹⁵, M Losada¹⁶², P Loscutoff¹⁵, F Lo Sterzo^{132a,132b}, M J Losty^{159a,218}, X Lou⁴¹, A Lounis¹¹⁵, K F Loureiro¹⁶², J Love⁶, P A Love⁷¹, A J Lowe^{143,184}, F Lu^{33a}, H J Lubatti¹³⁸, C Luci^{132a,132b}, A Lucotte⁵⁵, A Ludwig⁴⁴, D Ludwig⁴², I Ludwig⁴⁸, J Ludwig⁴⁸, F Luehring⁶⁰, G Luijckx¹⁰⁵, W Lukas⁶¹, L Luminari^{132a}, E Lund¹¹⁷, B Lund-Jensen¹⁴⁷, B Lundberg⁷⁹, J Lundberg^{146a,146b}, O Lundberg^{146a,146b}, J Lundquist³⁶, M Lungwitz⁸¹, D Lynn²⁵, E Lytken⁷⁹, H Ma²⁵, L L Ma¹⁷³, G Maccarrone⁴⁷, A Macchiolo⁹⁹, B Maček⁷⁴, J Machado Miguens^{124a}, R Mackeprang³⁶, R J Madaras¹⁵, H J Maddocks⁷¹, W F Mader⁴⁴, R Maenner^{58c}, T Maeno²⁵, P Mättig¹⁷⁵, S Mättig⁸¹, L Magnoni¹⁶³, E Magradze⁵⁴, K Mahboubi⁴⁸, J Mahlstedt¹⁰⁵, S Mahmoud⁷³, G Mahout¹⁸, C Maiani¹³⁶, C Maidantchik^{24a}, A Maio^{124a,180}, S Majewski²⁵, Y Makida⁶⁵, N Makovec¹¹⁵, P Mal¹³⁶, B Malaescu³⁰, Pa Malecki³⁹, P Malecki³⁹, V P Maleev¹²¹, F Malek⁵⁵, U Mallik⁶², D Malon⁶, C Malone¹⁴³, S Maltezos¹⁰, V Malyshev¹⁰⁷, S Malyukov³⁰, R Mameghani⁹⁸, J Mamuzic^{13b}, A Manabe⁶⁵, L Mandelli^{89a}, I Mandić⁷⁴, R Mandrysch¹⁶, J Maneira^{124a}, A Manfredini⁹⁹, P S Mangeard⁸⁸, L Manhaes de Andrade Filho^{24b}, J A Manjarres Ramos¹³⁶, A Mann⁵⁴, P M Manning¹³⁷, A Manousakis-Katsikakis⁹, B Mansoulie¹³⁶, A Mapelli³⁰, L Mapelli³⁰, L March⁸⁰, J F Marchand²⁹, F Marchese^{133a,133b}, G Marchiori⁷⁸, M Marcisovsky¹²⁵, C P Marino¹⁶⁹, F Marroquim^{24a}, Z Marshall³⁰, F K Martens¹⁵⁸, L F Marti¹⁷, S Marti-Garcia¹⁶⁷, B Martin³⁰, B Martin⁸⁸, J P Martin⁹³, T A Martin¹⁸, V J Martin⁴⁶, B Martin dit Latour⁴⁹, S Martin-Haugh¹⁴⁹, M Martinez¹², V Martinez Outschoorn⁵⁷, A C Martyniuk¹⁶⁹, M Marx⁸², F Marzano^{132a}, A Marzin¹¹¹, L Masetti⁸¹, T Mashimo¹⁵⁵, R Mashinistov⁹⁴, J Masik⁸², A L Maslennikov¹⁰⁷, I Massa^{20a,20b}, G Massaro¹⁰⁵, N Massol⁵, P Mastrandrea¹⁴⁸,

A Mastroberardino^{37a,37b}, T Masubuchi¹⁵⁵, P Matricon¹¹⁵, H Matsunaga¹⁵⁵, T Matsushita⁶⁶, C Mattravers^{118,181}, J Maurer⁸³, S J Maxfield⁷³, A Mayne¹³⁹, R Mazini¹⁵¹, M Mazur²¹, L Mazzaferro^{133a,133b}, M Mazzanti^{89a}, J Mc Donald⁸⁵, S P Mc Kee⁸⁷, A McCarn¹⁶⁵, R L McCarthy¹⁴⁸, T G McCarthy²⁹, N A McCubbin¹²⁹, K W McFarlane^{56,218}, J A Mcfayden¹³⁹, G Mchedlidze^{51b}, T McLaughlan¹⁸, S J McMahon¹²⁹, R A McPherson^{169,189}, A Meade⁸⁴, J Mechnich¹⁰⁵, M Mechtel¹⁷⁵, M Medinnis⁴², R Meera-Lebbai¹¹¹, T Meguro¹¹⁶, R Mehdiyev⁹³, S Mehlhase³⁶, A Mehta⁷³, K Meier^{58a}, B Meirose⁷⁹, C Melachrinou³¹, B R Mellado Garcia¹⁷³, F Meloni^{89a,89b}, L Mendoza Navas¹⁶², Z Meng^{151,199}, A Mengarelli^{20a,20b}, S Menke⁹⁹, E Meoni¹⁶¹, K M Mercurio⁵⁷, P Mermod⁴⁹, L Merola^{102a,102b}, C Meroni^{89a}, F S Merritt³¹, H Merritt¹⁰⁹, A Messina^{30,203}, J Metcalfe²⁵, A S Mete¹⁶³, C Meyer⁸¹, C Meyer³¹, J-P Meyer¹³⁶, J Meyer¹⁷⁴, J Meyer⁵⁴, T C Meyer³⁰, J Miao^{33d}, S Michal³⁰, L Micu^{26a}, R P Middleton¹²⁹, S Migas⁷³, L Mijović¹³⁶, G Mikenberg¹⁷², M Mikestikova¹²⁵, M Mikuž⁷⁴, D W Miller³¹, R J Miller⁸⁸, W J Mills¹⁶⁸, C Mills⁵⁷, A Milov¹⁷², D A Milstead^{146a,146b}, D Milstein¹⁷², A A Minaenko¹²⁸, M Miñano Moya¹⁶⁷, I A Minashvili⁶⁴, A I Mincer¹⁰⁸, B Mindur³⁸, M Mineev⁶⁴, Y Ming¹⁷³, L M Mir¹², G Mirabelli^{132a}, J Mitrevski¹³⁷, V A Mitsou¹⁶⁷, S Mitsui⁶⁵, P S Miyagawa¹³⁹, J U Mjörnmark⁷⁹, T Moa^{146a,146b}, V Moeller²⁸, K Mönig⁴², N Möser²¹, S Mohapatra¹⁴⁸, W Mohr⁴⁸, R Moles-Valls¹⁶⁷, A Molfetas³⁰, J Monk⁷⁷, E Monnier⁸³, J Montejo Berlingen¹², F Monticelli⁷⁰, S Monzani^{20a,20b}, R W Moore³, G Moorhead⁸⁶, C Mora Herrera⁴⁹, A Moraes⁵³, N Morange¹³⁶, J Morel⁵⁴, G Morello^{37a,37b}, D Moreno⁸¹, M Moreno Llácer¹⁶⁷, P Morettini^{50a}, M Morgenstern⁴⁴, M Morii⁵⁷, A K Morley³⁰, G Mornacchi³⁰, J D Morris⁷⁵, L Morvaj¹⁰¹, H G Moser⁹⁹, M Mosidze^{51b}, J Moss¹⁰⁹, R Mount¹⁴³, E Mountricha^{10,204}, S V Mouraviev^{94,218}, E J W Moyse⁸⁴, F Mueller^{58a}, J Mueller¹²³, K Mueller²¹, T A Müller⁹⁸, T Mueller⁸¹, D Muenstermann³⁰, Y Munwes¹⁵³, W J Murray¹²⁹, I Mussche¹⁰⁵, E Musto^{102a,102b}, A G Myagkov¹²⁸, M Myska¹²⁵, J Nadal¹², K Nagai¹⁶⁰, R Nagai¹⁵⁷, K Nagano⁶⁵, A Nagarkar¹⁰⁹, Y Nagasaka⁵⁹, M Nagel⁹⁹, A M Nairz³⁰, Y Nakahama³⁰, K Nakamura¹⁵⁵, T Nakamura¹⁵⁵, I Nakano¹¹⁰, G Nanava²¹, A Napier¹⁶¹, R Narayan^{58b}, M Nash^{77,181}, T Nattermann²¹, T Naumann⁴², G Navarro¹⁶², H A Neal⁸⁷, P Yu Nechaeva⁹⁴, T J Neep⁸², A Negri^{119a,119b}, G Negri³⁰, M Negrini^{20a}, S Nektarijevic⁴⁹, A Nelson¹⁶³, T K Nelson¹⁴³, S Nemecek¹²⁵, P Nemethy¹⁰⁸, A A Nepomuceno^{24a}, M Nessi^{30,205}, M S Neubauer¹⁶⁵, M Neumann¹⁷⁵, A Neusiedl⁸¹, R M Neves¹⁰⁸, P Nevski²⁵, F M Newcomer¹²⁰, P R Newman¹⁸, V Nguyen Thi Hong¹³⁶, R B Nickerson¹¹⁸, R Nicolaidou¹³⁶, B Nicquevert³⁰, F Niedercorn¹¹⁵, J Nielsen¹³⁷, N Nikiforou³⁵, A Nikiforov¹⁶, V Nikolaenko¹²⁸, I Nikolic-Audit⁷⁸, K Nikolics⁴⁹, K Nikolopoulos¹⁸, H Nilsen⁴⁸, P Nilsson⁸, Y Ninomiya¹⁵⁵, A Nisati^{132a}, R Nisius⁹⁹, T Nobe¹⁵⁷, L Nodulman⁶, M Nomachi¹¹⁶, I Nomidis¹⁵⁴, S Norberg¹¹¹, M Nordberg³⁰, P R Norton¹²⁹, J Novakova¹²⁶, M Nozaki⁶⁵, L Nozka¹¹³, I M Nugent^{159a}, A-E Nuncio-Quiroz²¹, G Nunes Hanninger⁸⁶, T Nunnemann⁹⁸, E Nurse⁷⁷, B J O'Brien⁴⁶, D C O'Neil¹⁴², V O'Shea⁵³, L B Oakes⁹⁸, F G Oakham^{29,183}, H Oberlack⁹⁹, J Ocariz⁷⁸, A Ochi⁶⁶, S Oda⁶⁹, S Odaka⁶⁵, J Odier⁸³, H Ogren⁶⁰, A Oh⁸², S H Oh⁴⁵, C C Ohm³⁰, T Ohshima¹⁰¹, H Okawa²⁵, Y Okumura³¹, T Okuyama¹⁵⁵, A Olariu^{26a}, A G Olchevski⁶⁴, S A Olivares Pino^{32a}, M Oliveira^{124a,186}, D Oliveira Damazio²⁵, E Oliver Garcia¹⁶⁷, D Olivito¹²⁰, A Olszewski³⁹, J Olszowska³⁹, A Onofre^{124a,206}, P U E Onyisi³¹, C J Oram^{159a}, M J Oreglia³¹, Y Oren¹⁵³, D Orestano^{134a,134b}, N Orlando^{72a,72b}, I Orlov¹⁰⁷, C Oropeza Barrera⁵³, R S Orr¹⁵⁸, B Osculati^{50a,50b}, R Ospanov¹²⁰, C Osuna¹², G Otero y Garzon²⁷, J P Ottersbach¹⁰⁵, M Ouchrif^{135d}, E A Ouellette¹⁶⁹, F Ould-Saada¹¹⁷, A Ouraou¹³⁶, Q Ouyang^{33a}, A Ovcharova¹⁵, M Owen⁸², S Owen¹³⁹, V E Ozcan^{19a}, N Ozturk⁸, A Pacheco Pages¹², C Padilla Aranda¹², S Pagan Griso¹⁵, E Paganis¹³⁹, C Pahl⁹⁹, F Paige²⁵, P Pais⁸⁴, K Pajchel¹¹⁷, G Palacino^{159b}, C P Paleari⁷, S Palestini³⁰, D Pallin³⁴,

A Palma^{124a}, J D Palmer¹⁸, Y B Pan¹⁷³, E Panagiotopoulou¹⁰, P Pani¹⁰⁵, N Panikashvili⁸⁷, S Panitkin²⁵, D Pantea^{26a}, A Papadelis^{146a}, Th D Papadopoulou¹⁰, A Paramonov⁶, D Paredes Hernandez³⁴, W Park^{25,207}, M A Parker²⁸, F Parodi^{50a,50b}, J A Parsons³⁵, U Parzefall⁴⁸, S Pashapour⁵⁴, E Pasqualucci^{132a}, S Passaggio^{50a}, A Passeri^{134a}, F Pastore^{134a,134b,218}, Fr Pastore⁷⁶, G Pásztor^{49,208}, S Pataria¹⁷⁵, N Patel¹⁵⁰, J R Pater⁸², S Patricelli^{102a,102b}, T Pauly³⁰, M Pecsý^{144a}, S Pedraza Lopez¹⁶⁷, M I Pedraza Morales¹⁷³, S V Peleganchuk¹⁰⁷, D Pelikan¹⁶⁶, H Peng^{33b}, B Penning³¹, A Penson³⁵, J Penwell⁶⁰, M Perantoni^{24a}, K Perez^{35,209}, T Perez Cavalcanti⁴², E Perez Codina^{159a}, M T Pérez García-Estañ¹⁶⁷, V Perez Reale³⁵, L Perini^{89a,89b}, H Pernegger³⁰, R Perrino^{72a}, P Perrodo⁵, V D Peshekhonov⁶⁴, K Peters³⁰, B A Petersen³⁰, J Petersen³⁰, T C Petersen³⁶, E Petit⁵, A Petridis¹⁵⁴, C Petridou¹⁵⁴, E Petrolo^{132a}, F Petrucci^{134a,134b}, D Petschull⁴², M Petteni¹⁴², R Pezoa^{32b}, A Phan⁸⁶, P W Phillips¹²⁹, G Piacquadio³⁰, A Picazio⁴⁹, E Piccaro⁷⁵, M Piccinini^{20a,20b}, S M Piec⁴², R Piegai²⁷, D T Pignotti¹⁰⁹, J E Pilcher³¹, A D Pilkington⁸², J Pina^{124a,180}, M Pinamonti^{164a,164c}, A Pinder¹¹⁸, J L Pinfold³, B Pinto^{124a}, C Pizio^{89a,89b}, M Plamondon¹⁶⁹, M-A Pleier²⁵, E Plotnikova⁶⁴, A Poblaguev²⁵, S Poddar^{58a}, F Podlyski³⁴, L Poggioli¹¹⁵, D Pohl²¹, M Pohl⁴⁹, G Polesello^{119a}, A Policicchio^{37a,37b}, A Polini^{20a}, J Poll⁷⁵, V Polychronakos²⁵, D Pomeroy²³, K Pommès³⁰, L Pontecorvo^{132a}, B G Pope⁸⁸, G A Popeneciu^{26a}, D S Popovic^{13a}, A Poppleton³⁰, X Portell Bueso³⁰, G E Pospelov⁹⁹, S Pospisil¹²⁷, I N Potrap⁹⁹, C J Potter¹⁴⁹, C T Potter¹¹⁴, G Poulard³⁰, J Poveda⁶⁰, V Pozdnyakov⁶⁴, R Prabhu⁷⁷, P Pralavorio⁸³, A Pranko¹⁵, S Prasad³⁰, R Pravahan²⁵, S Prell⁶³, K Pretzl¹⁷, D Price⁶⁰, J Price⁷³, L EPrice⁶, D Prieur¹²³, M Primavera^{72a}, K Prokofiev¹⁰⁸, F Prokoshin^{32b}, S Protopopescu²⁵, J Proudfoot⁶, X Prudent⁴⁴, M Przybycien³⁸, H Przysiezniak⁵, S Psoroulas²¹, E Ptacek¹¹⁴, E Pueschel⁸⁴, J Purdham⁸⁷, M Purohit^{25,207}, P Puzo¹¹⁵, Y Pylypchenko⁶², J Qian⁸⁷, A Quadt⁵⁴, D R Quarrie¹⁵, W B Quayle¹⁷³, F Quinonez^{32a}, M Raas¹⁰⁴, V Radeka²⁵, V Radescu⁴², P Radloff¹¹⁴, T Rador^{19a}, F Ragusa^{89a,89b}, G Rahal¹⁷⁸, A M Rahimi¹⁰⁹, D Rahm²⁵, S Rajagopalan²⁵, M Rammensee⁴⁸, M Rammes¹⁴¹, A S Randle-Conde⁴⁰, K Randrianarivony²⁹, F Rauscher⁹⁸, T C Rave⁴⁸, M Raymond³⁰, A L Read¹¹⁷, D M Rebuzzi^{119a,119b}, A Redelbach¹⁷⁴, G Redlinger²⁵, R Reece¹²⁰, K Reeves⁴¹, E Reinherz-Aronis¹⁵³, A Reinsch¹¹⁴, I Reisinger⁴³, C Rembser³⁰, Z L Ren¹⁵¹, A Renaud¹¹⁵, M Rescigno^{132a}, S Resconi^{89a}, B Resende¹³⁶, P Reznicek⁹⁸, R Rezvani¹⁵⁸, R Richter⁹⁹, E Richter-Was^{5,210}, M Ridel⁷⁸, M Rijpstra¹⁰⁵, M Rijssenbeek¹⁴⁸, A Rimoldi^{119a,119b}, L Rinaldi^{20a}, R R Rios⁴⁰, I Riu¹², G Rivoltella^{89a,89b}, F Rizatdinova¹¹², E Rizvi⁷⁵, S H Robertson^{85,189}, A Robichaud-Veronneau¹¹⁸, D Robinson²⁸, J E M Robinson⁸², A Robson⁵³, J G Rocha de Lima¹⁰⁶, C Roda^{122a,122b}, D Roda Dos Santos³⁰, A Roe⁵⁴, S Roe³⁰, O Røhne¹¹⁷, S Rolli¹⁶¹, A Romaniouk⁹⁶, M Romano^{20a,20b}, G Romeo²⁷, E RomeroAdam¹⁶⁷, N Rompotis¹³⁸, L Roos⁷⁸, E Ros¹⁶⁷, S Rosati^{132a}, K Rosbach⁴⁹, A Rose¹⁴⁹, M Rose⁷⁶, G A Rosenbaum¹⁵⁸, E I Rosenberg⁶³, P L Rosendahl¹⁴, O Rosenthal¹⁴¹, L Rosselet⁴⁹, V Rossetti¹², E Rossi^{132a,132b}, L P Rossi^{50a}, M Rotaru^{26a}, I Roth¹⁷², J Rothberg¹³⁸, D Rousseau¹¹⁵, C R Royon¹³⁶, A Rozanov⁸³, Y Rozen¹⁵², X Ruan^{33a,211}, F Rubbo¹², I Rubinskiy⁴², N Ruckstuhl¹⁰⁵, V I Rud⁹⁷, C Rudolph⁴⁴, G Rudolph⁶¹, F Rühr⁷, A Ruiz-Martinez⁶³, L Rumyantsev⁶⁴, Z Rurikova⁴⁸, N A Rusakovich⁶⁴, J P Rutherford⁷, C Ruwiedel^{15,218}, P Ruzicka¹²⁵, Y F Ryabov¹²¹, M Rybar¹²⁶, G Rybkin¹¹⁵, N C Ryder¹¹⁸, A F Saavedra¹⁵⁰, I Sadeh¹⁵³, H F-W Sadrozinski¹³⁷, R Sadykov⁶⁴, F Safai Tehrani^{132a}, H Sakamoto¹⁵⁵, G Salamanna⁷⁵, A Salamon^{133a}, M Saleem¹¹¹, D Salek³⁰, D Salihagic⁹⁹, A Salnikov¹⁴³, J Salt¹⁶⁷, B M Salvachua Ferrando⁶, D Salvatore^{37a,37b}, F Salvatore¹⁴⁹, A Salvucci¹⁰⁴, A Salzburger³⁰, D Sampsonidis¹⁵⁴, B H Samset¹¹⁷, A Sanchez^{102a,102b}, V Sanchez Martinez¹⁶⁷, H Sandaker¹⁴, H G Sander⁸¹, M P Sanders⁹⁸, M Sandhoff¹⁷⁵, T Sandoval²⁸, C Sandoval¹⁶²,

R Sandstroem⁹⁹, D P C Sankey¹²⁹, A Sansoni⁴⁷, C Santamarina Rios⁸⁵, C Santoni³⁴, R Santonico^{133a,133b}, H Santos^{124a}, J G Saraiva^{124a}, T Sarangi¹⁷³, E Sarkisyan-Grinbaum⁸, F Sarri^{122a,122b}, G Sartisohn¹⁷⁵, O Sasaki⁶⁵, Y Sasaki¹⁵⁵, N Sasao⁶⁷, I Satsounkevitch⁹⁰, G Sauvage^{5,218}, E Sauvan⁵, J B Sauvan¹¹⁵, P Savard^{158,183}, V Savinov¹²³, D O Savu³⁰, L Sawyer^{25,191}, D H Saxon⁵³, J Saxon¹²⁰, C Sbarra^{20a}, A Sbrizzi^{20a,20b}, D A Scannicchio¹⁶³, M Scarcella¹⁵⁰, J Schaarschmidt¹¹⁵, P Schacht⁹⁹, D Schaefer¹²⁰, U Schäfer⁸¹, S Schaepe²¹, S Schaetzel^{58b}, A C Schaffer¹¹⁵, D Schaile⁹⁸, R D Schamberger¹⁴⁸, A G Schamov¹⁰⁷, V Scharf^{58a}, V A Schegelsky¹²¹, D Scheirich⁸⁷, M Schernau¹⁶³, M I Scherzer³⁵, C Schiavi^{50a,50b}, J Schieck⁹⁸, M Schioppa^{37a,37b}, S Schlenker³⁰, E Schmidt⁴⁸, K Schmieden²¹, C Schmitt⁸¹, S Schmitt^{58b}, M Schmitz²¹, B Schneider¹⁷, U Schnoor⁴⁴, A Schoening^{58b}, A L S Schorlemmer⁵⁴, M Schott³⁰, D Schouten^{159a}, J Schovancova¹²⁵, M Schram⁸⁵, C Schroeder⁸¹, N Schroer^{58c}, M J Schultens²¹, J Schultes¹⁷⁵, H-C Schultz-Coulon^{58a}, H Schulz¹⁶, M Schumacher⁴⁸, B A Schumm¹³⁷, Ph Schune¹³⁶, C Schwanenberger⁸², A Schwartzman¹⁴³, Ph Schwegler⁹⁹, Ph Schwemling⁷⁸, R Schwienhorst⁸⁸, R Schwierz⁴⁴, J Schwindling¹³⁶, T Schwindt²¹, M Schwoerer⁵, G Sciolla²³, W G Scott¹²⁹, J Searcy¹¹⁴, G Sedov⁴², E Sedykh¹²¹, S C Seidel¹⁰³, A Seiden¹³⁷, F Seifert⁴⁴, J M Seixas^{24a}, G Sekhniaidze^{102a}, S J Sekula⁴⁰, K E Selbach⁴⁶, D M Seliverstov¹²¹, B Sellden^{146a}, G Sellers⁷³, M Seman^{144b}, N Semprini-Cesari^{20a,20b}, C Serfon⁹⁸, L Serin¹¹⁵, L Serkin⁵⁴, R Seuster⁹⁹, H Severini¹¹¹, A Sfyrila³⁰, E Shabalina⁵⁴, M Shamim¹¹⁴, L Y Shan^{33a}, J T Shank²², Q T Shao⁸⁶, M Shapiro¹⁵, P B Shatalov⁹⁵, K Shaw^{164a,164c}, D Sherman¹⁷⁶, P Sherwood⁷⁷, S Shimizu¹⁰¹, M Shimojima¹⁰⁰, T Shin⁵⁶, M Shiyakova⁶⁴, A Shmeleva⁹⁴, M J Shochet³¹, D Short¹¹⁸, S Shrestha⁶³, E Shulga⁹⁶, M A Shupe⁷, P Sicho¹²⁵, A Sidoti^{132a}, F Siegert⁴⁸, Dj Sijacki^{13a}, O Silbert¹⁷², J Silva^{124a}, Y Silver¹⁵³, D Silverstein¹⁴³, S B Silverstein^{146a}, V Simak¹²⁷, O Simard¹³⁶, Lj Simic^{13a}, S Simion¹¹⁵, E Simioni⁸¹, B Simmons⁷⁷, R Simoniello^{89a,89b}, M Simonyan³⁶, P Sinervo¹⁵⁸, N B Sinev¹¹⁴, V Sipica¹⁴¹, G Siragusa¹⁷⁴, A Sircar²⁵, A N Sisakyan^{64,218}, S Yu Sivoklov⁹⁷, J Sjölin^{146a,146b}, T B Sjursen¹⁴, L A Skinnari¹⁵, H P Skottowe⁵⁷, K Skovpen¹⁰⁷, P Skubic¹¹¹, M Slater¹⁸, T Slavicek¹²⁷, K Sliwa¹⁶¹, V Smakhtin¹⁷², B H Smart⁴⁶, L Smestad¹¹⁷, S Yu Smirnov⁹⁶, Y Smirnov⁹⁶, L N Smirnova⁹⁷, O Smirnova⁷⁹, B C Smith⁵⁷, D Smith¹⁴³, K M Smith⁵³, M Smizanska⁷¹, K Smolek¹²⁷, A A Snesarev⁹⁴, S W Snow⁸², J Snow¹¹¹, S Snyder²⁵, R Sobie^{169,189}, J Sodomka¹²⁷, A Soffer¹⁵³, C A Solans¹⁶⁷, M Solar¹²⁷, J Solc¹²⁷, E Yu Soldatov⁹⁶, U Soldevila¹⁶⁷, E Solfaroli Camillocci^{132a,132b}, A A Solodkov¹²⁸, O V Solovyanov¹²⁸, V Solovyev¹²¹, N Soni¹, V Sopko¹²⁷, B Sopko¹²⁷, M Sosebee⁸, R Soualah^{164a,164c}, A Soukharev¹⁰⁷, S Spagnolo^{72a,72b}, F Spanò⁷⁶, R Spighi^{20a}, G Spigo³⁰, R Spiwoks³⁰, M Spousta^{126,212}, T Spreitzer¹⁵⁸, B Spurlock⁸, R D St Denis⁵³, J Stahlman¹²⁰, R Stamen^{58a}, E Stanecka³⁹, R W Stanek⁶, C Stanescu^{134a}, M Stanescu-Bellu⁴², M M Stanitzki⁴², S Stapnes¹¹⁷, E A Starchenko¹²⁸, J Stark⁵⁵, P Staroba¹²⁵, P Starovoitov⁴², R Staszewski³⁹, A Staude⁹⁸, P Stavina^{144a,218}, G Steele⁵³, P Steinbach⁴⁴, P Steinberg²⁵, I Stekl¹²⁷, B Stelzer¹⁴², H J Stelzer⁸⁸, O Stelzer-Chilton^{159a}, H Stenzel⁵², S Stern⁹⁹, G A Stewart³⁰, J A Stillings²¹, M C Stockton⁸⁵, K Stoerig⁴⁸, G Stoicea^{26a}, S Stonjek⁹⁹, P Strachota¹²⁶, A R Stradling⁸, A Straessner⁴⁴, J Strandberg¹⁴⁷, S Strandberg^{146a,146b}, A Strandlie¹¹⁷, M Strang¹⁰⁹, E Strauss¹⁴³, M Strauss¹¹¹, P Strizenec^{144b}, R Ströhmer¹⁷⁴, D M Strom¹¹⁴, J A Strong^{76,218}, R Stroynowski⁴⁰, J Strube¹²⁹, B Stugu¹⁴, I Stumer^{25,218}, J Stupak¹⁴⁸, P Sturm¹⁷⁵, N A Styles⁴², D A Soh^{151,201}, D Su¹⁴³, H S Subramania³, A Succurro¹², Y Sugaya¹¹⁶, C Suhr¹⁰⁶, M Suk¹²⁶, V V Sulin⁹⁴, S Sultansoy^{4d}, T Sumida⁶⁷, X Sun⁵⁵, J E Sundermann⁴⁸, K Suruliz¹³⁹, G Susinno^{37a,37b}, M R Sutton¹⁴⁹, Y Suzuki⁶⁵, Y Suzuki⁶⁶, M Svatos¹²⁵, S Swedish¹⁶⁸, I Sykora^{144a}, T Sykora¹²⁶, J Sánchez¹⁶⁷, D Ta¹⁰⁵, K Tackmann⁴², A Taffard¹⁶³, R Tafirout^{159a}, N Taiblum¹⁵³, Y Takahashi¹⁰¹, H Takai²⁵, R Takashima⁶⁸,

H Takeda⁶⁶, T Takeshita¹⁴⁰, Y Takubo⁶⁵, M Talby⁸³, A Talyshev^{107,185}, M C Tamsett²⁵, K G Tan⁸⁶, J Tanaka¹⁵⁵, R Tanaka¹¹⁵, S Tanaka¹³¹, S Tanaka⁶⁵, A J Tanasijczuk¹⁴², K Tani⁶⁶, N Tannoury⁸³, S Tapprogge⁸¹, D Tardif¹⁵⁸, S Tarem¹⁵², F Tarrade²⁹, G F Tartarelli^{89a}, P Tas¹²⁶, M Tasevsky¹²⁵, E Tassi^{37a,37b}, M Tatarkhanov¹⁵, Y Tayalati^{135d}, C Taylor⁷⁷, F E Taylor⁹², G N Taylor⁸⁶, W Taylor^{159b}, M Teinturier¹¹⁵, F A Teischinger³⁰, M Teixeira Dias Castanheira⁷⁵, P Teixeira-Dias⁷⁶, K K Temming⁴⁸, H Ten Kate³⁰, P K Teng¹⁵¹, S Terada⁶⁵, K Terashi¹⁵⁵, J Terron⁸⁰, M Testa⁴⁷, R J Teuscher^{158,189}, J Therhaag²¹, T Theveneaux-Pelzer⁷⁸, S Thoma⁴⁸, J P Thomas¹⁸, E N Thompson³⁵, P D Thompson¹⁸, P D Thompson¹⁵⁸, A S Thompson⁵³, L A Thomsen³⁶, E Thomson¹²⁰, M Thomson²⁸, W M Thong⁸⁶, R P Thun⁸⁷, F Tian³⁵, M J Tibbetts¹⁵, T Tic¹²⁵, V O Tikhomirov⁹⁴, Y A Tikhonov^{107,185}, S Timoshenko⁹⁶, P Tipton¹⁷⁶, S Tisserant⁸³, T Todorov⁵, S Todorova-Nova¹⁶¹, B Toggerson¹⁶³, J Tojo⁶⁹, S Tokár^{144a}, K Tokushuku⁶⁵, K Tollefson⁸⁸, M Tomoto¹⁰¹, L Tompkins³¹, K Toms¹⁰³, A Tonoyan¹⁴, C Topfel¹⁷, N D Topilin⁶⁴, I Torchiani³⁰, E Torrence¹¹⁴, H Torres⁷⁸, E Torró Pastor¹⁶⁷, J Toth^{83,208}, F Touchard⁸³, D R Tovey¹³⁹, T Trefzger¹⁷⁴, L Tremblet³⁰, A Tricoli³⁰, I M Trigger^{159a}, S Trincas-Duvoid⁷⁸, M F Tripiana⁷⁰, N Triplett²⁵, W Trischuk¹⁵⁸, B Trocmé⁵⁵, C Troncon^{89a}, M Trotter-McDonald¹⁴², M Trzebinski³⁹, A Trzupek³⁹, C Tsarouchas³⁰, J C-L Tseng¹¹⁸, M Tsiakiris¹⁰⁵, P V Tsiarehka⁹⁰, D Tsionou^{5,213}, G Tsipolitis¹⁰, S Tsiskaridze¹², V Tsiskaridze⁴⁸, E G Tskhadadze^{51a}, I I Tsukerman⁹⁵, V Tsulaia¹⁵, J-W Tsung²¹, S Tsuno⁶⁵, D Tsybychev¹⁴⁸, A Tua¹³⁹, A Tudorache^{26a}, V Tudorache^{26a}, J M Tuggle³¹, M Turala³⁹, D Turecek¹²⁷, I Turk Cakir^{4e}, E Turlay¹⁰⁵, R Turra^{89a,89b}, P M Tuts³⁵, A Tykhonov⁷⁴, M Tylmad^{146a,146b}, M Tyndel¹²⁹, G Tzanakos⁹, K Uchida²¹, I Ueda¹⁵⁵, R Ueno²⁹, M Ugland¹⁴, M Uhlenbrock²¹, M Uhrmacher⁵⁴, F Ukegawa¹⁶⁰, G Unal³⁰, A Undrus²⁵, G Unel¹⁶³, Y Unno⁶⁵, D Urbaniec³⁵, P Urquijo²¹, G Usai⁸, M Uslenghi^{119a,119b}, L Vacavant⁸³, V Vacek¹²⁷, B Vachon⁸⁵, S Vahsen¹⁵, J Valenta¹²⁵, S Valentinetti^{20a,20b}, A Valero¹⁶⁷, S Valkar¹²⁶, E Valladolid Gallego¹⁶⁷, S Vallecorsa¹⁵², J A Valls Ferrer¹⁶⁷, R Van Berg¹²⁰, P C Van Der Deijl¹⁰⁵, R van der Geer¹⁰⁵, H van der Graaf¹⁰⁵, R Van Der Leeuw¹⁰⁵, E van der Poel¹⁰⁵, D van der Ster³⁰, N van Eldik³⁰, P van Gemmeren⁶, I van Vulpen¹⁰⁵, M Vanadia⁹⁹, W Vandelli³⁰, A Vaniachine⁶, P Vankov⁴², F Vannucci⁷⁸, R Vari^{132a}, E W Varnes⁷, T Varol⁸⁴, D Varouchas¹⁵, A Vartapetian⁸, K E Varvell¹⁵⁰, V I Vassilakopoulos⁵⁶, F Vazeille³⁴, T Vazquez Schroeder⁵⁴, G Vegni^{89a,89b}, J J Veillet¹¹⁵, F Veloso^{124a}, R Veness³⁰, S Veneziano^{132a}, A Ventura^{72a,72b}, D Ventura⁸⁴, M Venturi⁴⁸, N Venturi¹⁵⁸, V Vercesi^{119a}, M Verducci¹³⁸, W Verkerke¹⁰⁵, J C Vermeulen¹⁰⁵, A Vest⁴⁴, M C Vetterli^{142,183}, I Vichou¹⁶⁵, T Vickey^{145b,214}, O E Vickey Boeriu^{145b}, G H A Viehhauser¹¹⁸, S Viel¹⁶⁸, M Villa^{20a,20b}, M Villaplana Perez¹⁶⁷, E Vilucchi⁴⁷, M G Vinciter²⁹, E Vinek³⁰, V B Vinogradov⁶⁴, M Virchaux^{136,218}, J Virzi¹⁵, O Vitells¹⁷², M Viti⁴², I Vivarelli⁴⁸, F Vives Vaque³, S Vlachos¹⁰, D Vladioiu⁹⁸, M Vlasak¹²⁷, A Vogel²¹, P Vokac¹²⁷, G Volpi⁴⁷, M Volpi⁸⁶, G Volpini^{89a}, H von der Schmitt⁹⁹, H von Radziewski⁴⁸, E von Toerne²¹, V Vorobel¹²⁶, V Vorwerk¹², M Vos¹⁶⁷, R Voss³⁰, J H Vossebeld⁷³, N Vranjes¹³⁶, M Vranjes Milosavljevic¹⁰⁵, V Vrba¹²⁵, M Vreeswijk¹⁰⁵, T Vu Anh⁴⁸, R Vuillermet³⁰, I Vukotic³¹, W Wagner¹⁷⁵, P Wagner¹²⁰, H Wahlen¹⁷⁵, S Wahrmund⁴⁴, J Wakabayashi¹⁰¹, S Walch⁸⁷, J Walder⁷¹, R Walker⁹⁸, W Walkowiak¹⁴¹, R Wall¹⁷⁶, P Waller⁷³, B Walsh¹⁷⁶, C Wang⁴⁵, H Wang¹⁷³, H Wang^{33b,215}, J Wang¹⁵¹, J Wang⁵⁵, R Wang¹⁰³, S M Wang¹⁵¹, T Wang²¹, A Warburton⁸⁵, C P Ward²⁸, M Warsinsky⁴⁸, A Washbrook⁴⁶, C Wasicki⁴², I Watanabe⁶⁶, P M Watkins¹⁸, A T Watson¹⁸, I J Watson¹⁵⁰, M F Watson¹⁸, G Watts¹³⁸, S Watts⁸², A T Waugh¹⁵⁰, B M Waugh⁷⁷, M S Weber¹⁷, P Weber⁵⁴, A R Weidberg¹¹⁸, P Weigell⁹⁹, J Weingarten⁵⁴, C Weiser⁴⁸, P S Wells³⁰, T Wenaus²⁵, D Wendland¹⁶, Z Weng^{151,201}, T Wengler³⁰, S Wenig³⁰, N Wermes²¹, M Werner⁴⁸, P Werner³⁰, M Werth¹⁶³, M Wessels^{58a},

J Wetter¹⁶¹, C Weydert⁵⁵, K Whalen²⁹, S J Wheeler-Ellis¹⁶³, A White⁸, M J White⁸⁶, S White^{122a,122b}, S R Whitehead¹¹⁸, D Whiteson¹⁶³, D Whittington⁶⁰, F Wicek¹¹⁵, D Wicke¹⁷⁵, F J Wickens¹²⁹, W Wiedenmann¹⁷³, M Wielers¹²⁹, P Wienemann²¹, C Wiglesworth⁷⁵, L A M Wiik-Fuchs⁴⁸, P A Wijeratne⁷⁷, A Wildauer⁹⁹, M A Wildt^{42,197}, I Wilhelm¹²⁶, H G Wilkens³⁰, J Z Will⁹⁸, E Williams³⁵, H H Williams¹²⁰, W Willis³⁵, S Willocq⁸⁴, J A Wilson¹⁸, M G Wilson¹⁴³, A Wilson⁸⁷, I Wingerter-Seez⁵, S Winkelmann⁴⁸, F Winklmeier³⁰, M Wittgen¹⁴³, S J Wollstadt⁸¹, M W Wolter³⁹, H Wolters^{124a,186}, W C Wong⁴¹, G Wooden⁸⁷, B K Wosiek³⁹, J Wotschack³⁰, M J Woudstra⁸², K W Wozniak³⁹, K Wraight⁵³, M Wright⁵³, B Wrona⁷³, S L Wu¹⁷³, X Wu⁴⁹, Y Wu^{33b,216}, E Wulf³⁵, B M Wynne⁴⁶, S Xella³⁶, M Xiao¹³⁶, S Xie⁴⁸, C Xu^{33b,204}, D Xu¹³⁹, B Yabsley¹⁵⁰, S Yacoob^{145a,217}, M Yamada⁶⁵, H Yamaguchi¹⁵⁵, A Yamamoto⁶⁵, K Yamamoto⁶³, S Yamamoto¹⁵⁵, T Yamamura¹⁵⁵, T Yamanaka¹⁵⁵, J Yamaoka⁴⁵, T Yamazaki¹⁵⁵, Y Yamazaki⁶⁶, Z Yan²², H Yang⁸⁷, U K Yang⁸², Y Yang¹⁰⁹, Z Yang^{146a,146b}, S Yanush⁹¹, L Yao^{33a}, Y Yao¹⁵, Y Yasu⁶⁵, G V Ybeles Smit¹³⁰, J Ye⁴⁰, S Ye²⁵, M Yilmaz^{4c}, R Yoosoofmiya¹²³, K Yorita¹⁷¹, R Yoshida⁶, C Young¹⁴³, C J Young¹¹⁸, S Youssef²², D Yu²⁵, J Yu⁸, J Yu¹¹², L Yuan⁶⁶, A Yurkewicz¹⁰⁶, B Zabinski³⁹, R Zaidan⁶², A M Zaitsev¹²⁸, Z Zajacova³⁰, L Zanello^{132a,132b}, D Zanzi⁹⁹, A Zaytsev²⁵, C Zeitnitz¹⁷⁵, M Zeman¹²⁵, A Zemla³⁹, C Zendler²¹, O Zenin¹²⁸, T Ženiš^{144a}, Z Zinonos^{122a,122b}, S Zenz¹⁵, D Zerwas¹¹⁵, G Zevi della Porta⁵⁷, Z Zhan^{33d}, D Zhang^{33b,ak}, H Zhang⁸⁸, J Zhang⁶, X Zhang^{33d}, Z Zhang¹¹⁵, L Zhao¹⁰⁸, T Zhao¹³⁸, Z Zhao^{33b}, A Zhemchugov⁶⁴, J Zhong¹¹⁸, B Zhou⁸⁷, N Zhou¹⁶³, Y Zhou¹⁵¹, C G Zhu^{33d}, H Zhu⁴², J Zhu⁸⁷, Y Zhu^{33b}, X Zhuang⁹⁸, V Zhuravlov⁹⁹, D Zieminska⁶⁰, N I Zimin⁶⁴, R Zimmermann²¹, S Zimmermann²¹, S Zimmermann⁴⁸, M Ziolkowski¹⁴¹, R Zitoun⁵, L Živković³⁵, V V Zmouchko^{128,218}, G Zobernig¹⁷³, A Zoccoli^{20a,20b}, M zur Nedden¹⁶, V Zutshi¹⁰⁶ and L Zwalinski³⁰

¹ School of Chemistry and Physics, University of Adelaide, Adelaide, Australia

² Physics Department, SUNY Albany, Albany NY, USA

³ Department of Physics, University of Alberta, Edmonton AB, Canada

^{4a} Department of Physics, Ankara University, Ankara, Turkey

^{4b} Department of Physics, Dumlupinar University, Kutahya, Turkey

^{4c} Department of Physics, Gazi University, Ankara, Turkey

^{4d} Division of Physics, TOBB University of Economics and Technology, Ankara, Turkey

^{4e} Turkish Atomic Energy Authority, Ankara, Turkey

⁵ LAPP, CNRS/IN2P3 and Université de Savoie, Annecy-le-Vieux, France

⁶ High Energy Physics Division, Argonne National Laboratory, Argonne, IL, USA

⁷ Department of Physics, University of Arizona, Tucson, AZ, USA

⁸ Department of Physics, The University of Texas at Arlington, Arlington, TX, USA

⁹ Physics Department, University of Athens, Athens, Greece

¹⁰ Physics Department, National Technical University of Athens, Zografou, Greece

¹¹ Institute of Physics, Azerbaijan Academy of Sciences, Baku, Azerbaijan

¹² Institut de Física d'Altes Energies and Departament de Física de la Universitat Autònoma de Barcelona and ICREA, Barcelona, Spain

^{13a} Institute of Physics, University of Belgrade, Belgrade, Serbia

^{13b} Vinca Institute of Nuclear Sciences, University of Belgrade, Belgrade, Serbia

¹⁴ Department for Physics and Technology, University of Bergen, Bergen, Norway

¹⁵ Physics Division, Lawrence Berkeley National Laboratory and University of California, Berkeley, CA, USA

¹⁶ Department of Physics, Humboldt University, Berlin, Germany

- ¹⁷ Albert Einstein Center for Fundamental Physics and Laboratory for High Energy Physics, University of Bern, Bern, Switzerland
- ¹⁸ School of Physics and Astronomy, University of Birmingham, Birmingham, UK
- ^{19a} Department of Physics, Bogazici University, Istanbul, Turkey
- ^{19b} Division of Physics, Dogus University, Istanbul, Turkey
- ^{19c} Department of Physics Engineering, Gaziantep University, Gaziantep, Turkey
- ^{19d} Department of Physics, Istanbul Technical University, Istanbul, Turkey
- ^{20a} INFN Sezione di Bologna, Bologna, Italy
- ^{20b} Dipartimento di Fisica, Università di Bologna, Bologna, Italy
- ²¹ Physikalisches Institut, University of Bonn, Bonn, Germany
- ²² Department of Physics, Boston University, Boston, MA, USA
- ²³ Department of Physics, Brandeis University, Waltham, MA, USA
- ^{24a} Universidade Federal do Rio De Janeiro COPPE/EE/IF, Rio de Janeiro, Brazil
- ^{24b} Federal University of Juiz de Fora (UFJF), Juiz de Fora, Brazil
- ^{24c} Federal University of Sao Joao del Rei (UFSJ), Sao Joao del Rei, Brazil
- ^{24d} Instituto de Fisica, Universidade de Sao Paulo, Sao Paulo, Brazil
- ²⁵ Physics Department, Brookhaven National Laboratory, Upton, NY, USA
- ^{26a} National Institute of Physics and Nuclear Engineering, Bucharest, Romania
- ^{26b} University Politehnica Bucharest, Bucharest, Romania
- ^{26c} West University in Timisoara, Timisoara, Romania
- ²⁷ Departamento de Física, Universidad de Buenos Aires, Buenos Aires, Argentina
- ²⁸ Cavendish Laboratory, University of Cambridge, Cambridge, UK
- ²⁹ Department of Physics, Carleton University, Ottawa, ON, Canada
- ³⁰ CERN, Geneva, Switzerland
- ³¹ Enrico Fermi Institute, University of Chicago, Chicago, IL, USA
- ^{32a} Departamento de Física, Pontificia Universidad Católica de Chile, Santiago, Chile
- ^{32b} Departamento de Física, Universidad Técnica Federico Santa María, Valparaíso, Chile
- ^{33a} Institute of High Energy Physics, Chinese Academy of Sciences, Beijing, China
- ^{33b} Department of Modern Physics, University of Science and Technology of China, Anhui, China
- ^{33c} Department of Physics, Nanjing University, Jiangsu, China
- ^{33d} School of Physics, Shandong University, Shandong, China
- ^{33e} Physics Department, Shanghai Jiao Tong University, Shanghai, China
- ³⁴ Laboratoire de Physique Corpusculaire, Clermont Université and Université Blaise Pascal and CNRS/IN2P3, Clermont-Ferrand, France
- ³⁵ Nevis Laboratory, Columbia University, Irvington, NY, USA
- ³⁶ Niels Bohr Institute, University of Copenhagen, Kobenhavn, Denmark
- ^{37a} INFN Gruppo Collegato di Cosenza, Italy
- ^{37b} Dipartimento di Fisica, Università della Calabria, Arcavata di Rende, Italy
- ³⁸ AGH University of Science and Technology, Faculty of Physics and Applied Computer Science, Krakow, Poland
- ³⁹ The Henryk Niewodniczanski Institute of Nuclear Physics, Polish Academy of Sciences, Krakow, Poland
- ⁴⁰ Physics Department, Southern Methodist University, Dallas, TX, USA
- ⁴¹ Physics Department, University of Texas at Dallas, Richardson, TX, USA
- ⁴² DESY, Hamburg and Zeuthen, Germany

- ⁴³ Institut für Experimentelle Physik IV, Technische Universität Dortmund, Dortmund, Germany
- ⁴⁴ Institut für Kern- und Teilchenphysik, Technical University Dresden, Dresden, Germany
- ⁴⁵ Department of Physics, Duke University, Durham, NC, USA
- ⁴⁶ SUPA—School of Physics and Astronomy, University of Edinburgh, Edinburgh, UK
- ⁴⁷ INFN Laboratori Nazionali di Frascati, Frascati, Italy
- ⁴⁸ Fakultät für Mathematik und Physik, Albert-Ludwigs-Universität, Freiburg, Germany
- ⁴⁹ Section de Physique, Université de Genève, Geneva, Switzerland
- ^{50a} INFN Sezione di Genova, Italy
- ^{50b} Dipartimento di Fisica, Università di Genova, Genova, Italy
- ^{51a} E Andronikashvili Institute of Physics, Iv Javakhishvili Tbilisi State University, Tbilisi, Georgia
- ^{51b} High Energy Physics Institute, Tbilisi State University, Tbilisi, Georgia
- ⁵² II Physikalisches Institut, Justus-Liebig-Universität Giessen, Giessen, Germany
- ⁵³ SUPA—School of Physics and Astronomy, University of Glasgow, Glasgow, UK
- ⁵⁴ II Physikalisches Institut, Georg-August-Universität, Göttingen, Germany
- ⁵⁵ Laboratoire de Physique Subatomique et de Cosmologie, Université Joseph Fourier and CNRS/IN2P3 and Institut National Polytechnique de Grenoble, Grenoble, France
- ⁵⁶ Department of Physics, Hampton University, Hampton, VA, USA
- ⁵⁷ Laboratory for Particle Physics and Cosmology, Harvard University, Cambridge, MA, USA
- ^{58a} Kirchhoff-Institut für Physik, Ruprecht-Karls-Universität Heidelberg, Heidelberg, Germany
- ^{58b} Physikalisches Institut, Ruprecht-Karls-Universität Heidelberg, Heidelberg, Germany
- ^{58c} ZITI Institut für technische Informatik, Ruprecht-Karls-Universität Heidelberg, Mannheim, Germany
- ⁵⁹ Faculty of Applied Information Science, Hiroshima Institute of Technology, Hiroshima, Japan
- ⁶⁰ Department of Physics, Indiana University, Bloomington, IN, USA
- ⁶¹ Institut für Astro- und Teilchenphysik, Leopold-Franzens-Universität, Innsbruck, Austria
- ⁶² University of Iowa, Iowa City, IA, USA
- ⁶³ Department of Physics and Astronomy, Iowa State University, Ames, IA, USA
- ⁶⁴ Joint Institute for Nuclear Research, JINR Dubna, Dubna, Russia
- ⁶⁵ KEK, High Energy Accelerator Research Organization, Tsukuba, Japan
- ⁶⁶ Graduate School of Science, Kobe University, Kobe, Japan
- ⁶⁷ Faculty of Science, Kyoto University, Kyoto, Japan
- ⁶⁸ Kyoto University of Education, Kyoto, Japan
- ⁶⁹ Department of Physics, Kyushu University, Fukuoka, Japan
- ⁷⁰ Instituto de Física La Plata, Universidad Nacional de La Plata and CONICET, La Plata, Argentina
- ⁷¹ Physics Department, Lancaster University, Lancaster, UK
- ^{72a} INFN Sezione di Lecce, Italy
- ^{72b} Dipartimento di Matematica e Fisica, Università del Salento, Lecce, Italy
- ⁷³ Oliver Lodge Laboratory, University of Liverpool, Liverpool, UK
- ⁷⁴ Department of Physics, Jožef Stefan Institute and University of Ljubljana, Ljubljana, Slovenia
- ⁷⁵ School of Physics and Astronomy, Queen Mary University of London, London, UK
- ⁷⁶ Department of Physics, Royal Holloway University of London, Surrey, UK
- ⁷⁷ Department of Physics and Astronomy, University College London, London, UK

- ⁷⁸ Laboratoire de Physique Nucléaire et de Hautes Energies, UPMC and Université Paris-Diderot and CNRS/IN2P3, Paris, France
- ⁷⁹ Fysiska institutionen, Lunds universitet, Lund, Sweden
- ⁸⁰ Departamento de Física Teórica C-15, Universidad Autónoma de Madrid, Madrid, Spain
- ⁸¹ Institut für Physik, Universität Mainz, Mainz, Germany
- ⁸² School of Physics and Astronomy, University of Manchester, Manchester, UK
- ⁸³ CPPM, Aix-Marseille Université and CNRS/IN2P3, Marseille, France
- ⁸⁴ Department of Physics, University of Massachusetts, Amherst, MA, USA
- ⁸⁵ Department of Physics, McGill University, Montreal, QC, Canada
- ⁸⁶ School of Physics, University of Melbourne, Victoria, Australia
- ⁸⁷ Department of Physics, The University of Michigan, Ann Arbor, MI, USA
- ⁸⁸ Department of Physics and Astronomy, Michigan State University, East Lansing, MI, USA
- ^{89a} INFN Sezione di Milano, Italy
- ^{89b} Dipartimento di Fisica, Università di Milano, Milano, Italy
- ⁹⁰ B I Stepanov Institute of Physics, National Academy of Sciences of Belarus, Minsk, Republic of Belarus
- ⁹¹ National Scientific and Educational Centre for Particle and High Energy Physics, Minsk, Republic of Belarus
- ⁹² Department of Physics, Massachusetts Institute of Technology, Cambridge, MA, USA
- ⁹³ Group of Particle Physics, University of Montreal, Montreal, QC, Canada
- ⁹⁴ P N Lebedev Institute of Physics, Academy of Sciences, Moscow, Russia
- ⁹⁵ Institute for Theoretical and Experimental Physics (ITEP), Moscow, Russia
- ⁹⁶ Moscow Engineering and Physics Institute (MEPhI), Moscow, Russia
- ⁹⁷ Skobeltsyn Institute of Nuclear Physics, Lomonosov Moscow State University, Moscow, Russia
- ⁹⁸ Fakultät für Physik, Ludwig-Maximilians-Universität München, München, Germany
- ⁹⁹ Max-Planck-Institut für Physik (Werner-Heisenberg-Institut), München, Germany
- ¹⁰⁰ Nagasaki Institute of Applied Science, Nagasaki, Japan
- ¹⁰¹ Graduate School of Science and Kobayashi-Maskawa Institute, Nagoya University, Nagoya, Japan
- ^{102a} INFN Sezione di Napoli, Italy
- ^{102b} Dipartimento di Scienze Fisiche, Università di Napoli, Napoli, Italy
- ¹⁰³ Department of Physics and Astronomy, University of New Mexico, Albuquerque, NM, USA
- ¹⁰⁴ Institute for Mathematics, Astrophysics and Particle Physics, Radboud University, Nijmegen/Nikhef, Nijmegen, Netherlands
- ¹⁰⁵ Nikhef National Institute for Subatomic Physics and University of Amsterdam, Amsterdam, Netherlands
- ¹⁰⁶ Department of Physics, Northern Illinois University, DeKalb, IL, USA
- ¹⁰⁷ Budker Institute of Nuclear Physics, SB RAS, Novosibirsk, Russia
- ¹⁰⁸ Department of Physics, New York University, New York, NY, USA
- ¹⁰⁹ Ohio State University, Columbus, OH, USA
- ¹¹⁰ Faculty of Science, Okayama University, Okayama, Japan
- ¹¹¹ Homer L. Dodge Department of Physics and Astronomy, University of Oklahoma, Norman, OK, USA
- ¹¹² Department of Physics, Oklahoma State University, Stillwater, OK, USA
- ¹¹³ Palacký University, RCPTM, Olomouc, Czech Republic

- ¹¹⁴ Center for High Energy Physics, University of Oregon, Eugene, OR, USA
- ¹¹⁵ LAL, Université Paris-Sud and CNRS/IN2P3, Orsay, France
- ¹¹⁶ Graduate School of Science, Osaka University, Osaka, Japan
- ¹¹⁷ Department of Physics, University of Oslo, Oslo, Norway
- ¹¹⁸ Department of Physics, Oxford University, Oxford, UK
- ^{119a} INFN Sezione di Pavia, Italy
- ^{119b} Dipartimento di Fisica, Università di Pavia, Pavia, Italy
- ¹²⁰ Department of Physics, University of Pennsylvania, Philadelphia, PA, USA
- ¹²¹ Petersburg Nuclear Physics Institute, Gatchina, Russia
- ^{122a} INFN Sezione di Pisa, Italy
- ^{122b} Dipartimento di Fisica Enrico Fermi, Università di Pisa, Pisa, Italy
- ¹²³ Department of Physics and Astronomy, University of Pittsburgh, Pittsburgh, PA, USA
- ^{124a} Laboratório de Instrumentação e Física Experimental de Partículas—LIP, Lisboa, Portugal
- ^{124b} Departamento de Física Teórica y del Cosmos and CAFPE, Universidad de Granada, Granada, Spain
- ¹²⁵ Institute of Physics, Academy of Sciences of the Czech Republic, Praha, Czech Republic
- ¹²⁶ Faculty of Mathematics and Physics, Charles University in Prague, Praha, Czech Republic
- ¹²⁷ Czech Technical University in Prague, Praha, Czech Republic
- ¹²⁸ State Research Center Institute for High Energy Physics, Protvino, Russia
- ¹²⁹ Particle Physics Department, Rutherford Appleton Laboratory, Didcot, UK
- ¹³⁰ Physics Department, University of Regina, Regina, SK, Canada
- ¹³¹ Ritsumeikan University, Kusatsu, Shiga, Japan
- ^{132a} INFN Sezione di Roma I, Italy
- ^{132b} Dipartimento di Fisica, Università La Sapienza, Roma, Italy
- ^{133a} INFN Sezione di Roma Tor Vergata, Italy
- ^{133b} Dipartimento di Fisica, Università di Roma Tor Vergata, Roma, Italy
- ^{134a} INFN Sezione di Roma Tre, Italy
- ^{134b} Dipartimento di Fisica, Università Roma Tre, Roma, Italy
- ^{135a} Faculté des Sciences Ain Chock, Réseau Universitaire de Physique des Hautes Energies—Université Hassan II, Casablanca, Morocco
- ^{135b} Centre National de l'Energie des Sciences Techniques Nucleaires, Rabat, Morocco
- ^{135c} Faculté des Sciences Semlalia, Université Cadi Ayyad, LPHEA-Marrakech, Morocco
- ^{135d} Faculté des Sciences, Université Mohamed Premier and LPTPM, Oujda, Morocco
- ^{135e} Faculté des Sciences, Université Mohammed V-Agdal, Rabat, Morocco
- ¹³⁶ DSM/IRFU (Institut de Recherches sur les Lois Fondamentales de l'Univers), CEA Saclay (Commissariat à l'Energie Atomique), Gif-sur-Yvette, France
- ¹³⁷ Santa Cruz Institute for Particle Physics, University of California Santa Cruz, Santa Cruz, CA, USA
- ¹³⁸ Department of Physics, University of Washington, Seattle, WA, USA
- ¹³⁹ Department of Physics and Astronomy, University of Sheffield, Sheffield, UK
- ¹⁴⁰ Department of Physics, Shinshu University, Nagano, Japan
- ¹⁴¹ Fachbereich Physik, Universität Siegen, Siegen, Germany
- ¹⁴² Department of Physics, Simon Fraser University, Burnaby, BC, Canada
- ¹⁴³ SLAC National Accelerator Laboratory, Stanford, CA, USA
- ^{144a} Faculty of Mathematics, Physics & Informatics, Comenius University, Bratislava, Slovak Republic

- ^{144b} Department of Subnuclear Physics, Institute of Experimental Physics of the Slovak Academy of Sciences, Kosice, Slovak Republic
- ^{145a} Department of Physics, University of Johannesburg, Johannesburg, South Africa
- ^{145b} School of Physics, University of the Witwatersrand, Johannesburg, South Africa
- ^{146a} Department of Physics, Stockholm University, Sweden
- ^{146b} The Oskar Klein Centre, Stockholm, Sweden
- ¹⁴⁷ Physics Department, Royal Institute of Technology, Stockholm, Sweden
- ¹⁴⁸ Departments of Physics & Astronomy and Chemistry, Stony Brook University, Stony Brook, NY, USA
- ¹⁴⁹ Department of Physics and Astronomy, University of Sussex, Brighton, UK
- ¹⁵⁰ School of Physics, University of Sydney, Sydney, Australia
- ¹⁵¹ Institute of Physics, Academia Sinica, Taipei, Taiwan
- ¹⁵² Department of Physics, Technion—Israel Institute of Technology, Haifa, Israel
- ¹⁵³ Raymond and Beverly Sackler School of Physics and Astronomy, Tel Aviv University, Tel Aviv, Israel
- ¹⁵⁴ Department of Physics, Aristotle University of Thessaloniki, Thessaloniki, Greece
- ¹⁵⁵ International Center for Elementary Particle Physics and Department of Physics, The University of Tokyo, Tokyo, Japan
- ¹⁵⁶ Graduate School of Science and Technology, Tokyo Metropolitan University, Tokyo, Japan
- ¹⁵⁷ Department of Physics, Tokyo Institute of Technology, Tokyo, Japan
- ¹⁵⁸ Department of Physics, University of Toronto, Toronto, ON, Canada
- ^{159a} TRIUMF, Vancouver, BC, Canada
- ^{159b} Department of Physics and Astronomy, York University, Toronto, ON, Canada
- ¹⁶⁰ Faculty of Pure and Applied Sciences, University of Tsukuba, Tsukuba, Japan
- ¹⁶¹ Department of Physics and Astronomy, Tufts University, Medford, MA, USA
- ¹⁶² Centro de Investigaciones, Universidad Antonio Narino, Bogota, Colombia
- ¹⁶³ Department of Physics and Astronomy, University of California Irvine, Irvine, CA, USA
- ^{164a} INFN Gruppo Collegato di Udine, Italy
- ^{164b} ICTP, Trieste, Italy
- ^{164c} Dipartimento di Chimica, Fisica e Ambiente, Università di Udine, Udine, Italy
- ¹⁶⁵ Department of Physics, University of Illinois, Urbana, IL, USA
- ¹⁶⁶ Department of Physics and Astronomy, University of Uppsala, Uppsala, Sweden
- ¹⁶⁷ Instituto de Física Corpuscular (IFIC) and Departamento de Física Atómica, Molecular y Nuclear and Departamento de Ingeniería Electrónica and Instituto de Microelectrónica de Barcelona (IMB-CNM), University of Valencia and CSIC, Valencia, Spain
- ¹⁶⁸ Department of Physics, University of British Columbia, Vancouver, BC, Canada
- ¹⁶⁹ Department of Physics and Astronomy, University of Victoria, Victoria, BC, Canada
- ¹⁷⁰ Department of Physics, University of Warwick, Coventry, UK
- ¹⁷¹ Waseda University, Tokyo, Japan
- ¹⁷² Department of Particle Physics, The Weizmann Institute of Science, Rehovot, Israel
- ¹⁷³ Department of Physics, University of Wisconsin, Madison, WI, USA
- ¹⁷⁴ Fakultät für Physik und Astronomie, Julius-Maximilians-Universität, Würzburg, Germany
- ¹⁷⁵ Fachbereich C Physik, Bergische Universität Wuppertal, Wuppertal, Germany
- ¹⁷⁶ Department of Physics, Yale University, New Haven, CT, USA
- ¹⁷⁷ Yerevan Physics Institute, Yerevan, Armenia
- ¹⁷⁸ Centre de Calcul de l'Institut National de Physique Nucléaire et de Physique des Particules (IN2P3), Villeurbanne, France

- ¹⁷⁹ Also at Laboratório de Instrumentação e Física Experimental de Partículas—LIP, Lisboa, Portugal
- ¹⁸⁰ Also at Faculdade de Ciências and CFNUL, Universidade de Lisboa, Lisboa, Portugal
- ¹⁸¹ Also at Particle Physics Department, Rutherford Appleton Laboratory, Didcot, UK
- ¹⁸² Also at Department of Physics, University of Johannesburg, Johannesburg, South Africa
- ¹⁸³ Also at TRIUMF, Vancouver, BC, Canada
- ¹⁸⁴ Also at Department of Physics, California State University, Fresno, CA, USA
- ¹⁸⁵ Also at Novosibirsk State University, Novosibirsk, Russia
- ¹⁸⁶ Also at Department of Physics, University of Coimbra, Coimbra, Portugal
- ¹⁸⁷ Also at Department of Physics, UASLP, San Luis Potosí, Mexico
- ¹⁸⁸ Also at Università di Napoli Parthenope, Napoli, Italy
- ¹⁸⁹ Also at Institute of Particle Physics (IPP), Canada
- ¹⁹⁰ Also at Department of Physics, Middle East Technical University, Ankara, Turkey
- ¹⁹¹ Also at Louisiana Tech University, Ruston, LA, USA
- ¹⁹² Also at Dep Física and CEFITEC of Faculdade de Ciências e Tecnologia, Universidade Nova de Lisboa, Caparica, Portugal
- ¹⁹³ Also at Department of Physics and Astronomy, University College London, London, UK
- ¹⁹⁴ Also at Group of Particle Physics, University of Montreal, Montreal, QC, Canada
- ¹⁹⁵ Also at Department of Physics, University of Cape Town, Cape Town, South Africa
- ¹⁹⁶ Also at Institute of Physics, Azerbaijan Academy of Sciences, Baku, Azerbaijan
- ¹⁹⁷ Also at Institut für Experimentalphysik, Universität Hamburg, Hamburg, Germany
- ¹⁹⁸ Also at Manhattan College, New York, NY, USA
- ¹⁹⁹ Also at School of Physics, Shandong University, Shandong, China
- ²⁰⁰ Also at CPPM, Aix-Marseille Université and CNRS/IN2P3, Marseille, France
- ²⁰¹ Also at School of Physics and Engineering, Sun Yat-sen University, Guanzhou, China
- ²⁰² Also at Academia Sinica Grid Computing, Institute of Physics, Academia Sinica, Taipei, Taiwan
- ²⁰³ Also at Dipartimento di Fisica, Università La Sapienza, Roma, Italy
- ²⁰⁴ Also at DSM/IRFU (Institut de Recherches sur les Lois Fondamentales de l'Univers), CEA Saclay (Commissariat à l'Energie Atomique), Gif-sur-Yvette, France
- ²⁰⁵ Also at section de Physique, Université de Genève, Geneva, Switzerland
- ²⁰⁶ Also at Departamento de Física, Universidade de Minho, Braga, Portugal
- ²⁰⁷ Also at Department of Physics and Astronomy, University of South Carolina, Columbia, SC, USA
- ²⁰⁸ Also at Institute for Particle and Nuclear Physics, Wigner Research Centre for Physics, Budapest, Hungary
- ²⁰⁹ Also at California Institute of Technology, Pasadena, CA, USA
- ²¹⁰ Also at Institute of Physics, Jagiellonian University, Krakow, Poland
- ²¹¹ Also at LAL, Université Paris-Sud and CNRS/IN2P3, Orsay, France
- ²¹² Also at Nevis Laboratory, Columbia University, Irvington, NY, USA
- ²¹³ Also at Department of Physics and Astronomy, University of Sheffield, Sheffield, UK
- ²¹⁴ Also at Department of Physics, Oxford University, Oxford, UK
- ²¹⁵ Also at Institute of Physics, Academia Sinica, Taipei, Taiwan
- ²¹⁶ Also at Department of Physics, The University of Michigan, Ann Arbor, MI, USA
- ²¹⁷ Also at Discipline of Physics, University of KwaZulu-Natal, Durban, South Africa
- ²¹⁸ Deceased

References

- [1] Randall L and Sundrum R 1999 A large mass hierarchy from a small extra dimension *Phys. Rev. Lett.* **83** 3370–3
- [2] Davoudiasl H, Hewett J L and Rizzo T G 2000 Phenomenology of the Randall–Sundrum gauge hierarchy model *Phys. Rev. Lett.* **84** 2080–3
- [3] ATLAS Collaboration 2012 Search for high-mass resonances decaying to dilepton final states in pp collisions at $\sqrt{s} = 7$ TeV with the ATLAS detector *J. High Energy Phys.* **JHEP11(2012)138**
- [4] CMS Collaboration 2012 Search for narrow resonances in dilepton mass spectra in pp collisions at $\sqrt{s} = 7$ TeV *Phys. Lett. B* **714** 158–79
- [5] Abazov V M *et al* (D0 Collaboration) 2010 Search for Randall–Sundrum gravitons in the dielectron and diphoton final states with 5.4 fb^{-1} of data from $p\bar{p}$ collisions at $\sqrt{s} = 1.96$ TeV *Phys. Rev. Lett.* **104** 241802
- [6] Aaltonen T *et al* (CDF Collaboration) 2011 Search for new dielectron resonances and Randall–Sundrum gravitons at the collider detector at Fermilab *Phys. Rev. Lett.* **107** 051801
- [7] Arkani–Hamed N, Dimopoulos S and Dvali G 1998 The hierarchy problem and new dimensions at a millimeter *Phys. Lett. B* **429** 263–72
- [8] Giudice G F, Rattazzi R and Wells J D 1999 Quantum gravity and extra dimensions at high-energy colliders *Nucl. Phys. B* **544** 3–38
- [9] Han T, Lykken J D and Zhang R-J 1999 On Kaluza–Klein states from large extra dimensions *Phys. Rev. D* **59** 105006
- [10] Hewett J L 1999 Indirect collider signals for extra dimensions *Phys. Rev. Lett.* **82** 4765–8
- [11] ATLAS Collaboration 2012 Search for extra dimensions using diphoton events in 7 TeV proton–proton collisions with the ATLAS detector *Phys. Lett. B* **710** 538–56
- [12] CMS Collaboration 2012 Search for signatures of extra dimensions in the diphoton mass spectrum at the large hadron collider *Phys. Rev. Lett.* **108** 111801
- [13] Adloff C *et al* (H1 Collaboration) 2003 Search for new physics in $e^{\pm}q$ contact interactions at HERA *Phys. Lett. B* **568** 35–47
- [14] Chekanov S *et al* (ZEUS Collaboration) 2004 Search for contact interactions, large extra dimensions and finite quark radius in ep collisions at HERA *Phys. Lett. B* **591** 23–41
- [15] Schael S *et al* (ALEPH Collaboration) 2007 Fermion pair production in e^+e^- collisions at 189–209 GeV and constraints on physics beyond the standard model *Eur. Phys. J. C* **49** 411–37
- [16] Abdallah J *et al* (DELPHI Collaboration) 2006 Measurement and interpretation of fermion-pair production at LEP energies above the Z resonance *Eur. Phys. J. C* **45** 589–632
- [17] LEP Working Group 2003 Combination of the LEP II $f\bar{f}$ results *LEP Working Group* LEP2FF/03-01 (<http://lepewwg.web.cern.ch/LEPEWWG/lep2/summer2003/Welcome.html>)
- [18] Abazov V *et al* (D0 Collaboration) 2009 Search for large extra spatial dimensions in the dielectron and diphoton channels in $p\bar{p}$ collisions at $\sqrt{s} = 1.96$ TeV *Phys. Rev. Lett.* **102** 051601
- [19] Abazov V *et al* (D0 Collaboration) 2009 Measurement of dijet angular distributions at $\sqrt{s} = 1.96$ TeV and searches for quark compositeness and extra spatial dimensions *Phys. Rev. Lett.* **103** 191803
- [20] ATLAS Collaboration 2008 The ATLAS experiment at the CERN large hadron collider *J. Instrum.* **3** S08003
- [21] ATLAS Collaboration 2011 Measurement of the inclusive isolated prompt photon cross section in pp collisions at $\sqrt{s} = 7$ TeV with the ATLAS detector *Phys. Rev. D* **83** 052005
- [22] ATLAS Collaboration 2011 Measurements of the photon identification efficiency with the ATLAS detector using 4.9 fb^{-1} of pp collision data collected in 2011 *ATLAS-CONF-2012-123* (<http://atlas.web.cern.ch/Atlas/GROUPS/PHYSICS/CONFNOTES/ATLAS-CONF-2012-123/>)
- [23] Lampl W, Laplace S, Lelas D, Loch P, Ma H, Menke S, Rajagopalan S, Rousseau D, Snyder S and Unal G Calorimeter clustering algorithms: description and performance *ATL-LARG-PUB-2008-002*. *ATL-COM-LARG-2008-003*
- [24] Cacciari M, Salam G P and Sapeta S 2010 On the characterisation of the underlying event *J. High Energy Phys.* **JHEP04(2010)065**

- [25] Sjostrand T, Lonnblad L and Mrenna S 2001 PYTHIA 6.2 physics and manual *Comput. Phys. Commun.* **135** 238
- [26] ATLAS Collaboration 2011 ATLAS tunes of PYTHIA 6 and PYTHIA 8 for MC11 *ATLAS-PHYS-PUB-2011-009* (<https://cdsweb.cern.ch/record/1363300>)
- [27] Gleisberg T, Hoeche S, Krauss F, Schonherr M, Schumann S, Siegert F and Winter J 2009 Event generation with SHERPA 1.1 *J. High Energy Phys.* **JHEP02(2009)007**
- [28] Agostinelli S *et al* (GEANT4 Collaboration) 2003 Geant4—a simulation toolkit *Nucl. Instrum. Methods A* **506** 250–303
- [29] ATLAS Collaboration 2010 The ATLAS simulation infrastructure *Eur. Phys. J. C* **70** 823–74
- [30] ATLAS Collaboration 2011 Luminosity determination in pp collisions at $\sqrt{s} = 7$ TeV using the ATLAS detector at the LHC *Eur. Phys. J. C* **71** 1630
- [31] Sherstnev A and Thorne R 2008 Parton distributions for LO generators *Eur. Phys. J. C* **55** 553–75
- [32] Binoth T, Guillet J, Pilon E and Werlen M 2000 A full next-to-leading order study of direct photon pair production in hadronic collisions *Eur. Phys. J. C* **16** 311–30
- [33] Martin A, Stirling W, Thorne R and Watt G 2009 Parton distributions for the LHC *Eur. Phys. J. C* **63** 189–285
- [34] Nadolsky P M, Lai H-L, Cao Q-H, Huston J, Pumplin J, Stump D, Tung W K and Yuan C P 2008 Implications of CTEQ global analysis for collider observables *Phys. Rev. D* **78** 013004
- [35] Kumar M, Mathews P, Ravindran V and Tripathi A 2009 Direct photon pair production at the LHC to order α_s in TeV scale gravity models *Nucl. Phys. B* **818** 28–51
- [36] Kumar M, Mathews P, Ravindran V and Tripathi A 2009 Diphoton signals in theories with large extra dimensions to NLO QCD at hadron colliders *Phys. Lett. B* **672** 45–50
- [37] Aaltonen T *et al* (CDF Collaboration) 2009 Search for new particles decaying into dijets in proton–antiproton collisions at $\sqrt{s} = 1.96$ TeV *Phys. Rev. D* **79** 112002
- [38] ATLAS Collaboration 2011 Search for dilepton resonances in pp collisions at $\sqrt{s} = 7$ TeV with the ATLAS detector *Phys. Rev. Lett.* **107** 272002
- [39] ATLAS Collaboration 2012 Search for new physics in the dijet mass distribution using 1 fb^{-1} of pp collision data at $\sqrt{s} = 7$ TeV collected by the ATLAS detector *Phys. Lett. B* **708** 37–54
- [40] ATLAS Collaboration 2012 Search for production of resonant states in the photon-jet mass distribution using pp collisions at $\sqrt{s} = 7$ TeV collected by the ATLAS detector *Phys. Rev. Lett.* **108** 211802
- [41] ATLAS Collaboration 2012 Measurement of the isolated diphoton cross section in pp collisions at $\sqrt{s} = 7$ TeV with the ATLAS detector *Phys. Rev. D* **85** 012003
- [42] ATLAS Collaboration 2011 Search for the standard model Higgs boson in the two photon decay channel with the ATLAS detector at the LHC *Phys. Lett. B* **705** 452–70
- [43] Choudalakis G and Casadei D 2012 Plotting the differences between data and expectation *Eur. Phys. J. Plus* **127** 25
- [44] Campbell J M, Ellis R K and Williams C 2011 Vector boson pair production at the LHC *J. High Energy Phys.* **JHEP07(2011)018**
- [45] ATLAS Collaboration 2011 Luminosity determination in pp collisions at $\sqrt{s} = 7$ TeV using the ATLAS detector in 2011 *ATLAS-CONF-2011-116* (<http://atlas.web.cern.ch/Atlas/GROUPS/PHYSICS/CONFNOTES/ATLAS-CONF-2011-116/>)
- [46] Choudalakis G 2011 On hypothesis testing, trials factor, hypertests and the BumpHunter arXiv:1101.0390 [physics.data-an]
- [47] Caldwell A, Kollar D and Kroninger K 2009 BAT—the Bayesian analysis toolkit *Comput. Phys. Commun.* **180** 2197–209
- [48] Allanach B, Odagiri K, Palmer M, Parker M A, Sabetfakhri A and Webber B R 2002 Exploring small extra dimensions at the large hadron collider *J. High Energy Phys.* **JHEP12(2002)039**
- [49] ATLAS Collaboration 2013 Search for contact interactions and large extra dimensions in dilepton events from pp collisions at $\sqrt{s} = 7$ TeV with the ATLAS detector *Phys. Rev. D* **87** 015010